Chattering Suppression Single Phase Variable Structure Controller for Mismatched Uncertain Interconnected Systems with Extended Perturbations

Cong-Trang Nguyen*, Nguyen Van Phuoc, Van-Duc Phan*****

** Power System Optimization Research Group, Faculty of Electrical and Electronics Engineering, Ton Duc Thang University, Ho Chi Minh City, Vietnam (e-mail: nguyencongtrang@tdtu.edu.vn).*
***Ho Chi Minh City Industry and Trade College, Ho Chi Minh City, Vietnam (e-mail: vanphuoc@hitu.edu.vn).*
****Faculty of Automotive Engineering, School of Engineering and Technology, Van Lang University, Ho Chi Minh City, Vietnam (email: duc.pv@vlu.edu.vn).*

Abstract: In this study, a chattering suppression single phase variable structure controller (CSSPVSC) is proposed for mismatched uncertain interconnected systems via a Moore-Penrose Inverse approach. Key achievements of this paper include: 1) a global stability of the subsystems is guaranteed by dismissing the reaching phase in conventional variable structure control (CVSC) and a chattering phenomenon in control input is effectively reduced by using tanh function; 2) an external perturbation is extended to the polynomial function of the state variables. Firstly, a reduce-order observer (ROO) is designed to estimate the unmeasurable state variables of the subsystems. Secondly, a ROO-based CSSPVSC is synthesized to force trajectories of each subsystem to a switching surface from an instance time. Next, an asymptotic stability condition of the whole system is ensured by employing the Lyapunov function together with the linear matrix inequality (LMI) theory. Finally, simulation results based on the MATLAB software are showed to demonstrate the proposed method effectiveness.

Keywords: variable structure control, reduced-order sliding mode observer, interconnected systems, chattering removal, single phase, extended disturbance.

1. INTRODUCTION

Variable structure control (VSC) with sliding mode, also called sliding mode control (SMC), is a well-known solution for handling linear systems with uncertain dynamics and external disturbances. Thanks are due to some distinguished features of the VSC such as finite-time convergence, fast dynamic response, good robustness, exogenous perturbations rejection ability, and its insensitivity to parameter variations. Numerous practical applications of VSC can be found in the fields such as electrical drives, electrical power systems, spacecraft, mobile robots, helicopters, etc. (Huynh et al., 2018; Salem et al., 2020; Soltanpour et al., 2020). Although the VSC in sliding mode has the significant achievements, in general, there are still two tasks that should be solved for SMC design. These involve:

1) Chattering phenomenon elimination: a new SMC design not only guarantees the system's global stability but also alleviates the high frequency oscillation in control signal.

2) Unknown exogenous perturbations: In this study, the external perturbations are extended with a more general function which comprises the polynomial function of the state variables. In the previous publications (Chung and Chang, 2011; Gao et al., 2019; Ghasemi et al., 2009; Shyu et al., 2000; Xue et al., 2015), the disturbances must be bounded by a known function of the outputs or a function of state variables.

For the above first task which should remove the influence of chattering in the VSC systems, there are lots of the published researches which applied the various methods to reduce or eliminate chattering. First, the chattering is reduced by using sign function added the control signal. In particular, a static output feedback variable structure controller based on the Razumikhin–Lyapunov approach was designed in (Yan et al., 2012) for a class of interconnected time-varying delay systems. In (Zheng and Yang, 2013), a decentralized sliding mode quantized controller based on the available states assumption was proposed for a class of uncertain nonlinear large-scale systems with dead zone nonlinearity in actuator devices. In (Gao et al., 2019), an integral sliding mode controller based on reduced-order observer (ROO) was investigated for a class of interconnected descriptor systems. However, these studies (Gao et al., 2019; Yan et al., 2012; Zheng and Yang, 2013) did not consider the mismatched uncertainty of subsystems and mismatched interconnections, and external disturbances. Another way to remove the chattering phenomenon is to replace a sign function by saturation function. Based on the approximation capability of multiplayer neural networks, a decentralized direct adaptive sliding mode controller was synthesized in (T. P. Zhang and Mei, 2006) for a class of large-scale systems with unknown function control gains and the high-order interconnections. In (Cheng and Chang, 2008), a decentralized adaptive sliding mode controller was developed for a class of multi-input and multi-output (MIMO) mismatched uncertain large-scale systems via the Lyapunov stability theory. An appropriate Lyapunov-Krasovskii functional-based adaptive variable structure neural controller was established for class of uncertain MIMO nonlinear systems with state time-varying delays and unknown nonlinear dead-zones (T. P. Zhang et al., 2009). By designing the multiple-sliding surface, the robust controller was developed in (Chung and Chang, 2011) for a class of decentralized multi-input large-scale systems. Nevertheless, the state variables of the plant in the works (Cheng and Chang, 2008; Chung and Chang, 2011; T. P. Zhang and Mei, 2006; T. P. Zhang et al., 2009) are assumed to be available. This is impossible in practice control system due to high sensor device costs or measurable inability. To solve this drawback, only output variables must be utilized in the controller design. For example, in (Koo et al., 2014), an asymptotic stabilization problem of a class of nonlinear large-scale systems was investigated by using decentralized output feedback fuzzy controller. In (Li and Zhang, 2019), an integral sliding mode controller was designed for Takagi-Sugeno fuzzy interconnected descriptor system under Lipschitz constraint. But the restrictions of these studies (Koo et al., 2014; Li and Zhang, 2019) are computation burden and structure complexity due to the full-order observer (FOO) with large dimension. This full-dimension model is not indispensable to execute. Next, the boundary layer design technique is one of the most common methods instead of a sign or saturation function. For instance, a continuous approximation of discontinuous control in the boundary layer is introduced in (Boiko, 2011) for a small linear system by the describing function, Popov, and the Poincare methods. Conversely, the boundary layer design has two main weaknesses which include the sacrifice of control accuracy and ineffective disturbance rejection ability. Another technique to hide discontinuity of control in its higher derivatives was implemented utilizing high-order sliding mode control (HOSMC) or second-order sliding mode control (SOSMC). For instance, an adaptive integral HOSMC was proposed in (Mondal and Mahanta, 2013) for small systems without external disturbances. In (Huynh et al., 2018), an adaptive SOSMC was explored for a class of complex interconnected systems. However, the norm of state variables in this study are bounded by positive scalar. In addition, major challenges of the HOSMC and SOSMC techniques include sensitivity to the unmodeled fast dynamics and inability to weaken chattering completely. Thus, it is essential for control systems to develop a novel ROO-based output feedback controller reducing the undesired chattering phenomenon.

For the above second task which will solve unknown external disturbances, this issue has been examined by recent researches (Ghasemi et al., 2009; Shi et al., 2018; Xue et al., 2015). In (Ghasemi et al., 2009), a decentralized adaptive controller was proposed to remove the chattering for a class of large-scale nonaffine nonlinear systems by using the tanh function. Based on this technique, an extended state observer-based a chattering free sliding mode control signal was established in (Shi et al., 2018) for a class of small systems. Nonetheless, the external perturbations in these publications (Ghasemi et al., 2009; Shi et al., 2018) are assumed to be positive constants. In (Xue et al., 2015), a decentralized adaptive integral sliding mode control law was synthesized by employing Barbalat's lemma for eliminating for nonlinear uncertain large-scale systems subject to known disturbances. Most recently, a decentralized controller based on FOO was investigated in (Ranjbar et al., 2020) for linear interconnected systems with unknown interconnections. However, this study has several restrictions which did not consider the mismatched uncertainty of subsystems, mismatched interconnection, and exogenous perturbations. Moreover, Authors in the above publications have used the CVSC technique which only yields the desired motion after sliding mode has happened. The system is invariant to the exogenous perturbations and uncertainties during the reaching phase and its performance is unknown in the reaching phase. For this reason, the whole stability and the robustness of the system may not be guaranteed or seriously pervert (Mantz et al., 2001). Consequently, it should be pointed out that the development of a novel variable structure control is necessary and urgent.

Inspired by the above observations, to the best of our knowledge, little devotion has been paid to getting the unwanted chattering removal and the system's global stability problems for complex interconnected systems, which is still open in the literature. In this work, we attempt to address a ROO-based CSSPVSC for the mismatched uncertain interconnected systems with extended perturbations. Firstly, a switching function is designed to remove the reaching phase in CVSC. The system's global stability is ensured and the system's desired dynamic behaviour is achieved from the beginning of its motion. Secondly, a new ROO is suggested to estimate the unmeasurable variables of the subsystems. Next, a novel CSSPVSC is constructed to dismiss the undesired high frequency fluctuation in control signal. Furthermore, the reduce order system in sliding mode is asymptotically stable under certain conditions by using well-known LMI method. Finally, by numerical example, the validity of the proposed ideas, techniques, and procedures are shown.

The structure of this study is planned as follows. The subsystem's description of a regular form and preliminaries are described in Section 2. Main achievements of this work are derived in Section 3, which contains a new ROO establishment, an asymptotical stability of the system, and a chattering reduction single phase VSC law. The proposed effectiveness is demonstrated by the simulation results in Section 4. Finally, some concluding remarks on the developed control strategy are outlined in Section 5.

2. PROBLEM PRELIMINARIES AND DESCRIPTION OF A REGULAR FORM

In this paper, we consider a general description of mismatched uncertain interconnected systems, which are compose of L-linked subsystems with extended perturbations. The mathematics model of each subsystem is described by following equations:

$$\begin{aligned}\dot{x}_i(t) &= \left[A_{ii} + \Delta A_{ii}(t)\right]x_i(t) + B_i\left[u_i(t) + f_i(x_i,\ t)\right] \\ &\quad + \sum_{\substack{j=1\\ j\neq i}}^{L}\left[K_{ij} + \Delta K_{ij}(t)\right]x_j(t), \qquad (1)\\ y_i(t) &= C_i x_i(t),\ i = 1, 2, ..., L,\end{aligned}$$

where $x_i \in R^{n_i}$, $u_i \in R^{m_i}$, and $y_i \in R^{p_i}$ with $m_i \le p_i < n_i$ are the state variables, the control input vectors, and output signals of the ith subsystem, respectively. The triples (A_{ii}, B_i, C_i) are constant matrices of appropriate dimensions. The matrix $K_{ij} \in R^{n_i \times p_j}$ corresponds to the interconnection of subsystems i and j. The matrices $\Delta A_{ii}(t)$ and $\Delta K_{ij}(t)$ show mismatched parameter uncertainties in the state matrix and mismatched uncertain interconnections with $\text{rank}[B_i : \Delta A_{ii} : \Delta K_{ij}] > \text{rank}(B_i) = m_i$. The term $f_i(x_i, t)$ is the disturbance input.

The following four assumptions are made for each subsystem.

Assumption 1. The pair (A_i, B_i) is completely controllable and the pair (C_i, A_i) is completely observable.

Assumption 2. The matrices B_i and C_i have full rank and $\text{rank}(C_i B_i) = m_i$.

Assumption 3. The mismatched uncertainties in state matrix of each isolated subsystem and in interconnection elements are supposed to satisfy $\Delta A_{ii}(t) = D_{ii}\Sigma_{ii}(x_i,t)E_{ii}$ and $\Delta K_{ij}(t) = G_{ij}\Sigma_{ij}(x_i,t)H_{ij}$, where D_{ii}, E_{ii}, G_{ij}, H_{ij} are any nonzero matrices of appropriate dimensions, and $\Sigma_{ii}(x_i,t)$, $\Sigma_{ij}(x_i,t)$ are unknown but respectively bounded as $\|\Sigma_{ii}(x_i,t)\| \le 1$, $\|\Sigma_{ij}(x_i,t)\| \le 1$ for all $(x_i,t) \in R^{n_i} \times R.$

Assumption 4. The exogenous disturbance $f_i(x_i,t)$ is bounded by the polynomial of $\|x_i\|$ with strictly positive coefficients:

$$\| f_i(x_i, t)\| \le \sum_{k=0}^{r} (\tilde{\varpi}_i)_k (\|x_i\|)^k, \tag{2}$$

where $(\tilde{\varpi}_i)_k$, $k = 0, 1, 2, ..., r$ are unknown positive constants. The positive integer r is determined by the designer in accordance with the knowledge about the order of the disturbances. For example, if the disturbances contain a term such as x_i^2, then one may choose $r = 2$.

For purpose of using single phase sliding mode technique, a switching function, $s_i(y_i(t),t) \in R^{m_i}$, is designed as follows

$$s_i(y_i(t),t) = \bar{s}_i(y_i,t) - \bar{s}_i(y_i,0)\exp(-\alpha_i t), \ i = 1, 2, ..., L, \tag{3}$$

where $\bar{s}_i(y_i,t) = T_i x_i = F_i C_i x_i = F_i y_i$ with $T_i \in R^{m_i \times n_i}$ and $F_i \in R^{m_i \times p_i}$. The matrix F_i should be properly chosen by the designer.

Remark 2.1. Standard assumptions 1-3 have been used in most existing publications (Huynh et al., 2018; Nguyen and Tsai, 2017). In assumption 2, $\text{rank}(C_i B_i) = m_i$ is a constraint of the triples (A_{ii}, B_i, C_i). This assumption ensures the existence of the output switching surface. In Assumption 4, an external disturbance is extended to the polynomial function of the state variables. That is, we consider a more general disturbance function than the perturbation function of the previous studies (Gao et al., 2019; Huynh et al., 2018; Xue et al., 2015).

Remark 2.2. The switching function (3) is extended to the concept of the variable structure control without reaching phase investigated in (Al-khazraji et al., 2011). In other words, the plant's trajectories always start from the switching surface and the desired dynamics response of the entire system always procure from the initial instance time. Thus, this will make the system more robust against disturbance than the CVSC.

Remark 2.3. The matrix T_i should fulfil all three properties mentioned in (Choi, 2007).

Now, to get a regular form of the subsystems, we use the Moore-Penrose inverse approach of the work (Choi, 2007). Assume that there exist symmetric matrices X_i, Y_i gratifying two constraints following LMIs:

$$\begin{aligned} &\Gamma_i X_i \Gamma_i + B_i Y_i B_i^T > 0, \\ &B_i^{\perp T}\left(A_i \Gamma_i X_i \Gamma_i + \Gamma_i Y_i \Gamma_i A_i^T\right) B_i^{\perp} < 0, \end{aligned} \tag{4}$$

where Γ_i and Γ_j are $n \times n$ symmetric matrices such that:

$$\Gamma_i = \begin{cases} I_i & \text{if } B_i^{\perp T} D_{ii} = 0, \\ I_i - E_{ii}^g E_{ii} & \text{otherwise,} \end{cases} \quad \Gamma_j = \begin{cases} I_j & \text{if } B_i^{\perp T} G_{ij} = 0, \\ I_j - H_{ij}^g H_{ij} & \text{otherwise,} \end{cases} \tag{5}$$

where E_{ii}^g and H_{ij}^g are the Moore-Penrose inverse of the matrix E_{ii} and H_{ij}, respectively, and $B_i^{\perp}$ is an orthogonal complement of the matrix B_i.

Remark 2.4. The terms $B_i^{\perp T} D_{ii} = 0$ and $B_i^{\perp T} G_{ij} = 0$, that is, the uncertainties of systems and the interconnection are matched. Otherwise, the terms $B_i^{\perp T} D_{ii} \ne 0$ and $B_i^{\perp T} G_{ij} \ne 0$, that is, the uncertainties of systems and the interconnection are mismatched.

Now, we factorise T_i in the form $T_i = R_i B_i^T Q_i^{-1}$, where R_i is a non-singular matrix, $Q_i = \Gamma_i X_i \Gamma_i + B_i Y_i B_i^T$, and consider a transformation matrix and its inverse as follows:

$$\bar{M}_i = \begin{bmatrix} B_i^{\perp T} \\ T_i \end{bmatrix} \text{ and } \bar{M}_i^{-1} = \left[Q_i B_i^{\perp} \left(B_i^{\perp T} Q_i B_i^{\perp} \right)^{-1} \ B_i \left(T_i B_i \right)^{-1} \right], \tag{6}$$

where $B_i^{\perp T} \in R^{(n_i - m_i) \times n_i}$.

Let be the state transformation

$$\begin{bmatrix} \vartheta_i(t) \\ \bar{s}_i(t) \end{bmatrix} = \bar{M}_i x_i(t), \tag{7}$$

where $\vartheta_i(t)$ and $\bar{s}_i(t)$ are the new state variables.

By combining the equations (1), (6), and (7), we can obtain the regular form below

$$\begin{aligned}
\dot{\vartheta}_i(t) &= \left[\bar{A}_{ii11}+\Delta\bar{A}_{ii11}\right]\vartheta_i(t)+\left[\bar{A}_{ii12}+\Delta\bar{A}_{ii12}\right]\bar{s}_i(t)\\
&\quad+\sum_{\substack{j=1\\ j\neq i}}^{L}\left\{\left[\bar{K}_{ij11}+\Delta\bar{K}_{ij11}\right]\vartheta_j(t)+\left[\bar{K}_{ij12}+\Delta\bar{K}_{ij12}\right]\bar{s}_j(t)\right\},\\
\dot{\bar{s}}_i(t) &= \left[\bar{A}_{ii21}+\Delta\bar{A}_{ii21}\right]\vartheta_i(t)+\left[\bar{A}_{ii22}+\Delta\bar{A}_{ii22}\right]\bar{s}_i(t)\\
&\quad+\left(T_iB_i\right)u_i(t)\ +\left(T_iB_i\right)f_i(x_i,t)\\
&\quad+\sum_{\substack{j=1\\ j\neq i}}^{L}\left\{\left[\bar{K}_{ij21}+\Delta\bar{K}_{ij21}\right]\vartheta_j(t)+\left[\bar{K}_{ij22}+\Delta\bar{K}_{ij22}\right]\bar{s}_j(t)\right\},
\end{aligned}\tag{8}$$

where

$$\begin{aligned}
\bar{A}_{ii11}+\Delta\bar{A}_{ii11} &= B_i^{\perp T}\left[A_{ii}+D_{ii}\Sigma_{ii}E_{ii}\right]Q_iB_i^{\perp}\left(B_i^{\perp T}Q_iB_i^{\perp}\right)^{-1},\\
\bar{A}_{ii12}+\Delta\bar{A}_{ii12} &= B_i^{\perp T}\left[A_{ii}+D_{ii}\Sigma_{ii}E_{ii}\right]B_i\left(T_iB_i\right)^{-1},\\
\bar{A}_{ii21}+\Delta\bar{A}_{ii21} &= R_iB_i^TQ_i^{-1}\left[A_{ii}+D_{ii}\Sigma_{ii}E_{ii}\right]Q_iB_i^{\perp}\left(B_i^{\perp T}Q_iB_i^{\perp}\right)^{-1},\\
\bar{A}_{ii22}+\Delta\bar{A}_{ii22} &= R_iB_i^TQ_i^{-1}\left[A_{ii}+D_{ii}\Sigma_{ii}E_{ii}\right]B_i\left(T_iB_i\right)^{-1},\\
\bar{K}_{ij11}+\Delta\bar{K}_{ij11} &= B_i^{\perp T}\left[K_{ij}+G_{ij}\Sigma_{ij}H_{ij}\right]Q_iB_i^{\perp}\left(B_i^{\perp T}Q_iB_i^{\perp}\right)^{-1},\\
\bar{K}_{ij12}+\Delta\bar{K}_{ij12} &= B_i^{\perp T}\left[K_{ij}+G_{ij}\Sigma_{ij}H_{ij}\right]B_i\left(T_iB_i\right)^{-1},\\
\bar{K}_{ij21}+\Delta\bar{K}_{ij21} &= T_i\left[K_{ij}+G_{ij}\Sigma_{ij}H_{ij}\right]Q_iB_i^{\perp}\left(B_i^{\perp T}Q_iB_i^{\perp}\right)^{-1},\\
\bar{K}_{ij22}+\Delta\bar{K}_{ij22} &= T_i\left[K_{ij}+G_{ij}\Sigma_{ij}H_{ij}\right]B_i\left(T_iB_i\right)^{-1},\\
\vartheta_i &= B_i^{\perp T}x_i,\ \text{and}\ \bar{s}_i=F_iy_i=T_ix_i.
\end{aligned}\tag{9}$$

From the results of the paper (Choi, 2007), we have

$$\begin{aligned}
\Delta\bar{A}_{ii11} &= B_i^{\perp T}D_{ii}\Sigma_{ii}(x_i,t)E_{ii}Q_iB_i^{\perp}\left(B_i^{\perp T}Q_iB_i^{\perp}\right)^{-1}=0,\\
\Delta\bar{K}_{ij11} &= B_i^{\perp T}G_{ij}\Sigma_{ij}(x_i,t)H_{ij}Q_iB_i^{\perp}\left(B_i^{\perp T}Q_iB_i^{\perp}\right)^{-1}=0,\\
\Delta\bar{A}_{ii21} &= R_iB_i^TQ_i^{-1}\left[D_{ii}\Sigma_{ii}(x_i,t)E_{ii}\right]Q_iB_i^{\perp}\left(B_i^{\perp T}Q_iB_i^{\perp}\right)^{-1}=0,\\
\Delta\bar{K}_{ij21} &= T_i\left[G_{ij}\Sigma_{ij}(x_i,t)H_{ij}\right]Q_iB_i^{\perp}\left(B_i^{\perp T}Q_iB_i^{\perp}\right)^{-1}=0.
\end{aligned}\tag{10}$$

By substituting (10) into (8), we can achieve a new regular form as below

$$\begin{aligned}
\dot{\vartheta}_i(t) &= \bar{A}_{ii11}\vartheta_i(t)+\left[\bar{A}_{ii12}+\Delta\bar{A}_{ii12}(t)\right]\bar{s}_i(t)\\
&\quad+\sum_{j=1,\,j\neq i}^{L}\left\{\bar{K}_{ij11}\vartheta_j(t)+\left[\bar{K}_{ij12}+\Delta\bar{K}_{ij12}(t)\right]\bar{s}_j(t)\right\},\\
\dot{\bar{s}}_i(t) &= \bar{A}_{ii21}\vartheta_i+\left[\bar{A}_{ii22}+\Delta\bar{A}_{ii22}\right]\bar{s}_i+\left(T_iB_i\right)\left[u_i+\right.\\
&\quad\left.f_i(x_i,t)\right]+\sum_{j=1,\,j\neq i}^{L}\left[\bar{K}_{ij21}\vartheta_j+\left[\bar{K}_{ij22}+\Delta\bar{K}_{ij22}\right]\bar{s}_j\right].
\end{aligned}\tag{11}$$

To elucidate the proof of the main results, a ROO that helps the controller design is first established in the following.

3. MAIN RESULTS

3.1 A novel reduced-order observer for uncertain interconnected systems

In this section, to estimate the unmeasurable states for the uncertain interconnected systems (1), we will establish a novel ROO. First, the new observer (12) with lower dimension is proposed to estimate the unmeasurable states:

$$\dot{\hat{\vartheta}}_i(t)=\bar{A}_{ii11}\hat{\vartheta}_i(t)+\bar{A}_{ii12}\bar{s}_i(t).\tag{12}$$

The block diagram of *i*th subsystem being structured by ROO (12) is showed in Figure 1. Now, we introduce an observer error of the *i*th subsystem as $\tilde{\vartheta}_i=\hat{\vartheta}_i-\vartheta_i$. By combining the first equation (11) and equation (12), we can achieve

$$\begin{aligned}
\dot{\tilde{\vartheta}}_i(t) &= \bar{A}_{ii11}\tilde{\vartheta}_i(t)-\Delta\bar{A}_{ii12}(t)\bar{s}_i(t)+\sum_{j=1,\,j\neq i}^{L}\left[\bar{K}_{ji11}\tilde{\vartheta}_i(t)\right]\\
&\quad-\sum_{j=1,\,j\neq i}^{L}\left[\bar{K}_{ji11}\hat{\vartheta}_i(t)+\bar{K}_{ji12}(t)\bar{s}_i(t)+\Delta\bar{K}_{ji12}(t)\bar{s}_i(t)\right].
\end{aligned}\tag{13}$$

Based on the equations (9) and (10), (13) becomes

$$\begin{aligned}
\dot{\tilde{\vartheta}}_i(t) &= \bar{A}_{ii11}\tilde{\vartheta}_i(t)-B_i^{\perp T}D_{ii}\Sigma_{ii}(x_i,t)E_{ii}B_i\left(T_iB_i\right)^{-1}\bar{s}_i(t)\\
&\quad+\sum_{j=1,\,j\neq i}^{L}\left[\bar{K}_{ji11}\tilde{\vartheta}_i\right]-\sum_{j=1,\,j\neq i}^{L}\left[\bar{K}_{ji11}\hat{\vartheta}_i+\bar{K}_{ji12}\bar{s}_i(t)\right]\\
&\quad-\sum_{j=1,\,j\neq i}^{L}\left[B_j^{\perp T}G_{ji}\Sigma_{ji}(x_j,t)H_{ji}B_j\left(T_jB_j\right)^{-1}\bar{s}_i(t)\right].
\end{aligned}\tag{14}$$

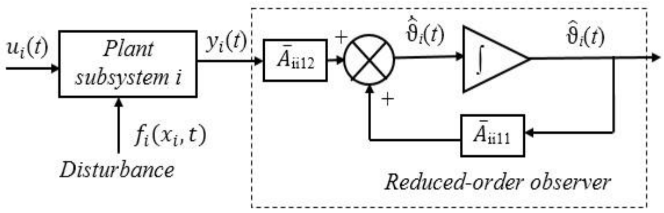

Fig. 1. The block diagram of the plant with ROO (12).

Remark 3.1. With the transformation matrix $\bar{M}_i$, the uncertain interconnected systems (1) is transformed into the regular form (11). Then, based on the regular form of the plant and the idea of the standard Luenberger observer design in (Luenberger, 1971), a new ROO (12) is designed to estimate the state variables of the original systems (1). It is worth mentioning that compared with the FOO (Koo et al., 2014), the ROO (12) with an (n_i-m_i)- dimensional dynamics will ensure that the conservatism is decreased and the robustness is enhanced. In addition, the observer error dynamics asymptotically approaches to zero in sliding mode. That is, the invariance property is guaranteed with this ROO.

Remark 3.2. From the obtained results in (Nguyen and Tsai, 2017), the matrix $\bar{A}_{ii11}$ is stable. Thus, the observer (12) and its estimate error dynamics (14) are asymptotically convergent to zero in the sliding mode.

With goal of the controller design, we now propose a new proposition for determining the upper bound of observer error.

Proposition 3.1. The norm of the estimated error $\left\|\tilde{\vartheta}_i(t)\right\|$ is bounded for all time by the solution $\tilde{\psi}_i$ of

$$\dot{\tilde{\psi}}_i(t) = \rho_i \tilde{\psi}_i + \bar{\gamma}_i \Big\{ \left\| B_i^{\perp T} D_{ii} \right\| \left\| E_{ii} B_i \left(T_i B_i \right)^{-1} \right\| + \sum_{j=1, j\neq i}^{L} \Big[\left\| B_j^{\perp T} G_{ji} \right\| \left\| H_{ji} B_j \left(T_j B_j \right)^{-1} \right\| + \left\| \bar{K}_{ji12} \right\| \Big] \left\| \bar{s}_i(t) \right\| + \sum_{j=1, j\neq i}^{L} \left\| \bar{K}_{ji11} \right\| \left\| \hat{\vartheta}_i(t) \right\| \Big\}, \ \tilde{\psi}_i(0) \geq \tilde{\varepsilon}_i \left\| \tilde{\vartheta}_i(0) \right\|, \quad (15)$$

where $\rho_i = \lambda_{\max_i} + \bar{\gamma}_i \sum_{j=1, j\neq i}^{L} \left\| \bar{K}_{ji11} \right\| < 0$, $\lambda_{\max_i}$ be the maximum eigenvalue of the stable matrix $\bar{A}_{ii11}$ and $\bar{\gamma}_i > 0$.

The proof of Proposition 3.1 can be found in Appendix A.

Now, we are in position to derive sufficient conditions by LMI such that the mismatched uncertain interconnected systems (1) is asymptotically stable in the sliding mode

3.2 Asymptotically stable condition by LMI

In this section, the stability analysis in sliding mode will be proved by applying the Lyapunov theory and the well-known LMI technique. Let us begin with considering the following LMI:

$$\begin{bmatrix} \Omega_i & \Psi_i \tilde{D}_{ii} & \tilde{E}_{ii}^T & \Psi_i \\ \tilde{D}_{ii}^T \Psi_i & -\varphi_i I_i & 0 & 0 \\ \tilde{E}_{ii} & 0 & -\varphi_i^{-1} I_i & 0 \\ \Psi_i & 0 & 0 & -(L-1)/\tilde{\gamma}_i \end{bmatrix} < 0, \quad (16)$$

where $\Omega_i = \bar{A}_{ii11}^T \Psi_i + \Psi_i \bar{A}_{ii11} + \sum_{j=1, j\neq i}^{L} (\tilde{\gamma}_j \bar{K}_{ji11}^T \bar{K}_{ji11} + \varphi_i^{-1} \Psi_i \tilde{G}_{ji} \tilde{G}_{ji}^T \Psi_i + \varphi_i \tilde{H}_{ji}^T \tilde{H}_{ji})$, $\tilde{D}_{ii} = B_i^{\perp T} D_{ii}$, $\tilde{E}_{ii} = E_{ii} Q_i B_i^{\perp} (B_i^{\perp T} Q_i B_i^{\perp})^{-1}$, $\tilde{G}_{ji} = B_j^{\perp T} G_{ji}$, $\tilde{H}_{ji} = H_{ji} Q_j B_j^{\perp} (B_j^{\perp T} Q_j B_j^{\perp})^{-1}$ are non-zero matrices, $\Psi_i \in R^{(n_i - m_i)\times(n_i - m_i)}$ is any positive matrix, φ_i, $\tilde{\gamma}_i$, and $\tilde{\gamma}_j$ are positive constants. Then, we will consider the following proposition.

Proposition 3.2. The solution of the first state-equation (8) is asymptotically stable in the sliding mode regime obtained with the switching function (3) if the LMI (16) has a feasible solution Ψ_i for some positive constants φ_i, $\tilde{\gamma}_i$ and $\tilde{\gamma}_j$.

The proof of Proposition 3.2 can be found in Appendix B.

Remark 3.3. The sufficient condition of the asymptotic stability in the LMI format (16) is easily solved via the LMI toolbox of MATLAB (Gahinet et al., 1994). This technique reduces the computation burden and the design complexity.

Remark 3.4. Compared to recent LMI approaches (Koo et al., 2014; Li and Zhang, 2019; Xue et al., 2015), the present LMI method indicates less number of matrix variables in LMI (16) and easily determines a feasible solution.

To continue the evaluation of new controller's efficacy, we will propose novel controllers by using Barbalat's lemma and tanh function in the following section.

3.3 Chattering suppression single phase VSC law design

In this section, we are going to determine the chattering free single phase sliding mode control laws such that the state trajectories of each subsystem will be driven to the switching surface (3) from the instance time and the chattering phenomenon in control input will be settled completely. The controllers will be designed based on the ROO (12).

First, assume the control law (17):

$$u_{1i}(t) = -\left(T_i B_i\right)^{-1} \tilde{\alpha}_i s_i - \left(T_i B_i\right)^{-1} \Big\{ \tilde{v}_{1i} \left(\left\| \hat{\vartheta}_i(t) \right\| + \tilde{\psi}_i(t) \right) + \sum_{j=1, j\neq i}^{L} \tilde{v}_{2i} \left(\left\| \hat{\vartheta}_i(t) \right\| + \tilde{\psi}_i(t) \right) + \sum_{j=1, j\neq i}^{L} \tilde{v}_{3i} \left\| \bar{s}_i \right\| + \tilde{v}_{4i} \left\| \bar{s}_i \right\| + \left\| \left(T_i B_i\right) \right\| \left\| f_i \right\| + \alpha_i \left\| F_i \right\| \left\| y_i(0) \right\| \exp(-\alpha_i t) \Big\} \frac{s_i}{\left\| s_i \right\|}, \quad (17)$$

where $\left\| f_i \right\| \leq \sum_{k=0}^{r} [(\varpi_{2_i})_k (\left\| Q_i B_i^{\perp} (B_i^{\perp T} Q_i B_i^{\perp})^{-1} \right\| (\left\| \hat{\vartheta}_i \right\| + \tilde{\psi}_i)) + \left\| B_i (T_i B_i)^{-1} \right\| \times \left\| F_i \right\| \left\| y_i \right\|)^k]$, $\tilde{\alpha}_i$, α_i are positive constants, the upper bound of the observer error $\tilde{\psi}_i(t)$ is solution of (15), and $\tilde{v}_{1i}$, $\tilde{v}_{2i}$, $\tilde{v}_{3i}$, $\tilde{v}_{4i}$ are control gains specified later.

Proposition 3.3. Suppose that the LMI (16) has a solution $\Psi_i > 0$. Consider the mismatched uncertain interconnected systems (1) subject to Assumptions 1-3. If the switching surface (3), the ROO (12), the CSSPVSC (17) are employed, and the observer error dynamics (14) satisfies Proposition 3.1, then the states of the system (1) will asymptotically converge to zero from the instance time under the proposed controller (17) and its control gains satisfy the following conditions

$$\begin{aligned} \tilde{v}_{1_i} &\geq \left\| \bar{A}_{ii21} \right\| + \left\| R_i B_i^T Q_i^{-1} D_{ii} \right\| \left\| E_{ii} Q_i B_i^{\perp} (B_i^{\perp T} Q_i B_i^{\perp})^{-1} \right\|, \\ \tilde{v}_{2_i} &\geq \left\| \bar{K}_{ji21} \right\| + \left\| T_j G_{ji} \right\| \left\| H_{ji} Q_j B_j^{\perp} (B_j^{\perp T} Q_j B_j^{\perp})^{-1} \right\|, \\ \tilde{v}_{3_i} &\geq \left\| \bar{K}_{ji22} \right\| + \left\| T_j G_{ji} \right\| \left\| H_{ji} B_j (T_j B_j)^{-1} \right\|, \\ \tilde{v}_{4_i} &\geq \left\| \bar{A}_{ii22} \right\| + \left\| R_i B_i^T Q_i^{-1} D_{ii} \right\| \left\| E_{ii} B_i (T_i B_i)^{-1} \right\|. \end{aligned} \quad (18)$$

The detailed proof of Proposition 3.3 is found in Appendix C.

Remark 3.5. Unlike existing related researches (Chung and Chang, 2011; Koo et al., 2014; Ranjbar et al., 2020), the single phase variable structure control strategy (17) that eliminates the reaching phase is proposed by using the ROO tool (12) and output information only. With this controller, the state trajectories of the subsystems will hit the switching surface (3) from the instance time $t \geq 0$ and the mismatched uncertain interconnected systems (1) is asymptotically stable in sliding mode. From the controller (17), we can see that the unit vector $(s_i / \left\| s_i \right\|)$ will induce the unwanted chattering in sliding mode.

In order to solve this problem, we will propose a new continuous time controller in the following proposition.

Proposition 3.4. By using the control law (19), the chattering in the control signals of interconnected systems (1) subjected to assumptions 1-3 will attenuate until they will vanish and the state will hit the switching surface from the zero reaching time, if the switching function is chosen as (3) and the control signal is proposed as follows:

$$u_{2i}(t) = -\left(T_iB_i\right)^{-1}\Big\{\bar{\nu}_{1i}\left[\left\|\hat{\vartheta}_i(t)\right\| + \tilde{\psi}_i(t)\right] + \sum_{j=1,\, j\neq i}^{L} \bar{\nu}_{2i} \times\left[\left\|\hat{\vartheta}_j(t)\right\| + \tilde{\psi}_j(t)\right] + \bar{\alpha}_i s_i + \tilde{\omega}_i(t)\frac{\|\theta_i\|}{\|\theta_i\| + \hat{\eta}_i e^{-\gamma_i t}}\Big\}, \tag{19}$$

where $\bar{\nu}_{1i} = \left\|\bar{A}_{ii21}\right\| + \left\|R_iB_i^TQ_i^{-1}D_{ii}\right\|\left\|E_{ii}Q_iB_i^{\perp}\left(B_i^{\perp T}Q_iB_i^{\perp}\right)^{-1}\right\|$,

$\bar{\nu}_{2i} = \left\|\bar{K}_{ji21}\right\| + \left\|T_jG_{ji}\right\|\left\|H_{ji}Q_jB_j^{\perp}\left(B_j^{\perp T}Q_jB_j^{\perp}\right)^{-1}\right\|$, $\bar{\alpha}_i$, $\hat{\eta}_i$, γ_i are positive constants, $\hat{\vartheta}_i$ is the state of observer (12), $\tilde{\psi}_i(t)$ is the upper bound of the observer error answered of (15), and

$$\begin{aligned}\tilde{\omega}_i(t) \geq{}& \sum_{j=1,\, j\neq i}^{L}\left[\left\|\bar{K}_{ji22}\right\| + \left\|T_jG_{ji}\right\|\left\|H_{ji}B_j\left(T_jB_j\right)^{-1}\right\|\right]\|F_i\|\|y_i\| \\ &+\left[\left\|\bar{A}_{ii22}\right\| + \left\|R_iB_i^TQ_i^{-1}D_{ii}\right\|\left\|E_{ii}B_i\left(T_iB_i\right)^{-1}\right\|\right]\|F_i\|\|y_i\| + \left\|\left(T_iB_i\right)\right\| \\ &\times\sum_{k=0}^{r}\left[\left(\tilde{\varpi}_{2_i}\right)_k\left(\left\|Q_iB_i^{\perp}\left(B_i^{\perp T}Q_iB_i^{\perp}\right)^{-1}\right\|\left(\left\|\hat{\vartheta}_i\right\| + \tilde{\psi}_i\right)\right.\right. \\ &\left.\left. + \left\|B_i\left(T_iB_i\right)^{-1}\right\|\|F_i\|\|y_i\|\right)^k\right] + \alpha_iF_iy_i(0)\exp(-\alpha_i t).\end{aligned} \tag{20}$$

The proof of Proposition 3.4 can be found in Appendix D.

Remark 3.6. From the above Proposition 3.4, it is undoubted that the proposed CSSPVSC (19) that utilizes the well-known Babalat lemma can mitigate the chattering phenomenon effectively for the mismatched uncertain interconnected systems with extended perturbations (1). However, using this technique, the state trajectories of the subsystems remains on the switching surface without to guarantee a finite-time convergence. This also is a limitation of this method.

Now, to solve this drawback, a new chattering free controller is proposed by using the tanh function as follows:

$$\begin{aligned}u_{3i}(t) ={}& -\left(T_iB_i\right)^{-1}\tilde{\alpha}_i s_i - \left(T_iB_i\right)^{-1}\Big\{\tilde{\nu}_{1i}\left(\left\|\hat{\vartheta}_i(t)\right\| + \tilde{\psi}_i(t)\right) \\ &+\sum_{j=1,\, j\neq i}^{L}\tilde{\nu}_{2i}\left(\left\|\hat{\vartheta}_i(t)\right\| + \tilde{\psi}_i(t)\right) + \sum_{j=1,\, j\neq i}^{L}\tilde{\nu}_{3i}\left\|\bar{s}_i\right\| + \tilde{\nu}_{4i}\left\|\bar{s}_i\right\| \\ &+\left\|\left(T_iB_i\right)\right\|\left\|f_i\right\| + \alpha_i\left\|F_i\right\|\left\|y_i(0)\right\|\exp(-\alpha_i t)\Big\}\tanh\left(s_i/\left\|s_i\right\|\right),\end{aligned} \tag{21}$$

where $\tilde{\nu}_{1i}$, $\tilde{\nu}_{2i}$, $\tilde{\nu}_{3i}$, $\tilde{\nu}_{4i}$ are control gains and defined in equation (18). The overall block diagrams of the proposed scheme that include the controlled system (1), ROO (12) are displayed in Figure 2 and 3 corresponding to the controllers (17) and (19), respectively. The design of the proposed control algorithm can be implemented as Figure 4.

Remark 3.7. According to the above controller (21), it is obvious that the undesired high frequency chattering in the control signal is alleviated, which will be demonstrated by the later simulation study in this paper. Concurrently, this controller also guarantees that the state trajectories of each subsystem are driven into the switching surface from the zero reaching time. That is, the restriction of the Proposition 3.3 is elucidated. Therefore, the chattering suppression controller (21) is very useful and more feasible, since it can be implemented in the practical control systems such as electrical motors and power systems, spacecraft, aircrafts, and flexible space structures, etc. (Salem et al., 2020; Soltanpour et al., 2020).

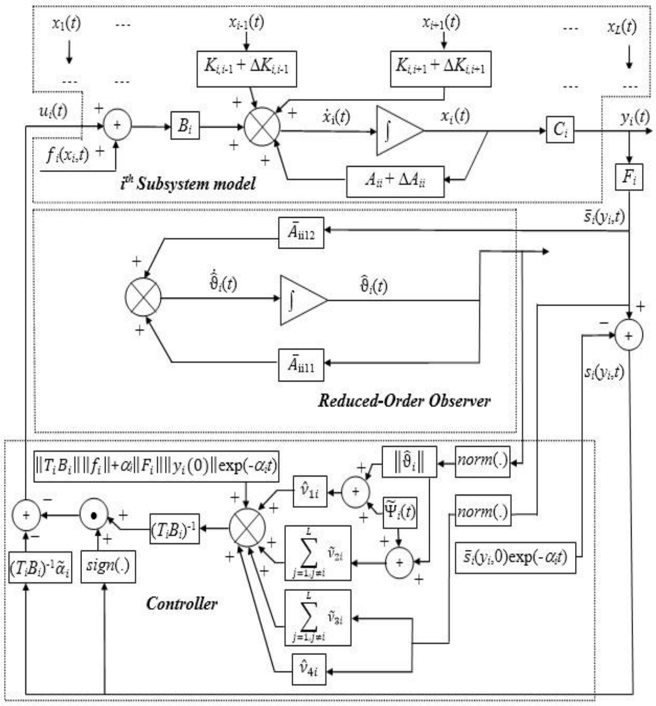

Fig. 2. Diagram of the *i*th subsystem when using controller (17).

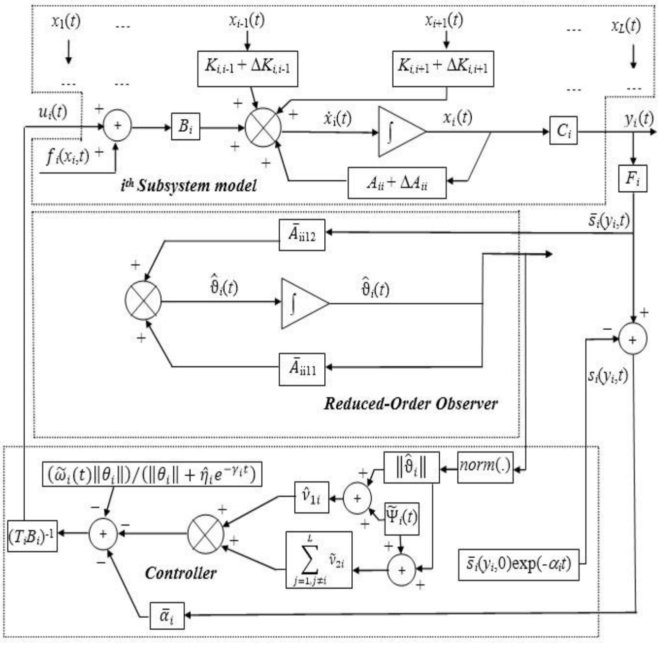

Fig. 3. Diagram of the *i*th subsystem when using controller (19).

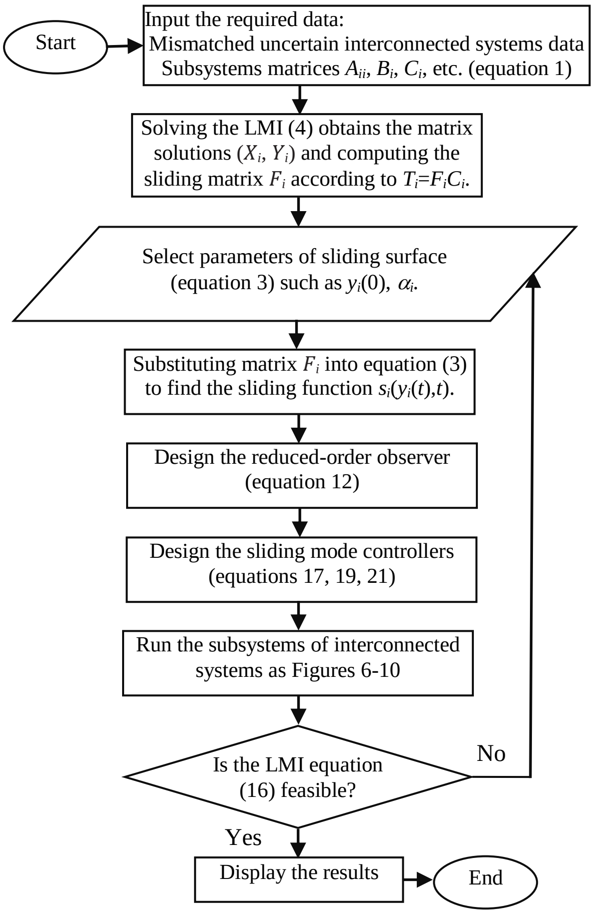

Fig. 4. The flowchart of the proposed ROO-based CSSPVSC.

4. ILLUSTRATIVE EXAMPLE

In the above section, we have gotten the main achievements comprising the ROO-based chattering-free single phase variable structure controllers and the whole system's stability in sliding mode. In this section, to emphasize the performance effectiveness of the proposed approaches, we develop a case study based on the example presented in (Lian and Zhao, 2009). Thus, we consider a system with $L = 2$, whose subsystem $i = 1$ has the Equation (22) $(n_1 = 3,\ m_1 = 2)$,

$$\begin{aligned}\dot{x}_1 &= \left[A_{11} + \Delta A_{11}(t)\right]x_1 + B_1\left[u_1(t) + f_1(x_1,\ t)\right] \\ &\quad + \left[K_{12} + \Delta K_{12}(t)\right]x_2(t),\ y_1 = C_1x_1,\end{aligned} \tag{22}$$

and subsystem $i = 2$ the Equation (23) $(n_2 = 3,\ m_2 = 2)$.

$$\begin{aligned}\dot{x}_2 &= \left[A_{22} + \Delta A_{22}(t)\right]x_2 + B_2\left[u_2(t) + f_2(x_2,\ t)\right] \\ &\quad + \left[K_{21} + \Delta K_{21}(t)\right]x_1(t),\ y_2 = C_2x_2.\end{aligned} \tag{23}$$

For the first subsystem, we have:

$$A_{11} = \begin{bmatrix} -1 & 1 & 0 \\ 0 & 1 & -1 \\ -1 & 1 & -0.75 \end{bmatrix},\ B_1 = \begin{bmatrix} 0 & 1 & 0.5 \end{bmatrix}^T,\ C_1 = \begin{bmatrix} 1 & 1 & -1 \\ 0 & 0 & 1 \end{bmatrix},$$

$$K_{12} = \begin{bmatrix} -0.2 & 0 & -0.1 \\ 0.1 & 0 & 0 \\ 0.2 & 0.1 & 0 \end{bmatrix},\ D_{11} = \begin{bmatrix} 0 \\ 0 \\ 1 \end{bmatrix},\ E_{11} = \begin{bmatrix} 1\ 1\ 0 \end{bmatrix},\ \Sigma_{11}(x_1,t) =$$

$0.17\sin(0.13t)$, $G_{12} = [0\ 1\ 0]^T$, $H_{12} = [1\ 1\ 0]$, $\Sigma_{12}(x_1,t) = 0.36\sin(0.15t)$, $\tilde{\varpi}_{10} = 0.011$, $\tilde{\varpi}_{11} = 0.017$, and $\tilde{\varpi}_{12} = 0.023$.

For the second subsystem, we have:

$$A_{22} = \begin{bmatrix} -0.1 & 1 & 0.2 \\ 1 & 1 & -1 \\ 0.5 & 1 & 0.1 \end{bmatrix},\ B_2 = \begin{bmatrix} 0 & 1 & -0.5 \end{bmatrix}^T,\ C_2 = \begin{bmatrix} 1 & 1 & 0 \\ 0 & 0 & 1 \end{bmatrix},$$

$$K_{21} = \begin{bmatrix} -0.2 & 0 & -0.1 \\ 0.1 & 0 & 0 \\ 0.2 & 0.1 & 0 \end{bmatrix},\ D_{22} = \begin{bmatrix} 0 \\ 0 \\ 1 \end{bmatrix},\ E_{22} = \begin{bmatrix} 1\ 1\ 0 \end{bmatrix},\ \Sigma_{22}(x_2,t) =$$

$0.18\sin(0.11t)$, $G_{21} = [0\ 1\ 0]^T$, $H_{21} = [1\ 1\ 0]$, $\Sigma_{21}(x_2,t) = 0.49\sin(0.32t)$, $\tilde{\varpi}_{20} = 0.015$, $\tilde{\varpi}_{21} = 0.021$, and $\tilde{\varpi}_{22} = 0.034$.

The block diagrams of the subsystems, including the proposed ROO and CSSPVSC, are given in Figure 5.

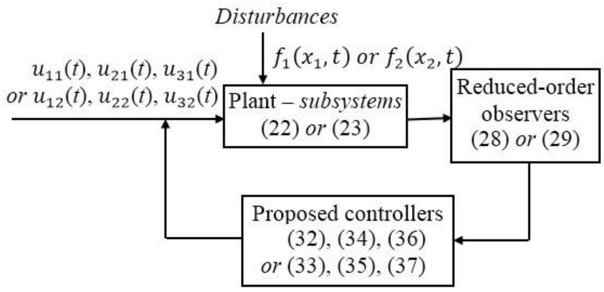

Fig. 5. Block diagram of the subsystems.

For this work, the initial conditions for two subsystems are selected to be $x_1(0) = x_2(0) = [1.72;\ -1.72;\ 0]^T$ and the following parameters are given as follows: $\alpha_1 = \alpha_2 = 0.015$, $\gamma_1 = \gamma_2 = 0.012$, and $\hat{\eta}_1 = \hat{\eta}_2 = 0.001$. By using the MATLAB's LMI Control Toolbox, the solutions of the LMIs constraints (4) embracing the symmetric matrices for two subsystems are solved as follows

$$X_1 = \begin{bmatrix} 37.1298 & -132.2244 & 15.2150 \\ -132.2244 & -300.4981 & 15.2879 \\ 15.2150 & 15.2879 & 1.3491 \end{bmatrix},\ Y_1 = \begin{bmatrix} 0.6238 \end{bmatrix}, \tag{24}$$

and

$$X_2 = \begin{bmatrix} 197.7259 & 132.5157 & -149.3973 \\ 132.5157 & 69.4260 & -149.5495 \\ -149.3973 & -149.5495 & 1.4154 \end{bmatrix},\ Y_2 = \begin{bmatrix} 0.3796 \end{bmatrix}. \tag{25}$$

The switching functions for each subsystem are exposed as

$$\begin{aligned}s_1(y_1(t),t) &= \begin{bmatrix} 1.6031 & -1.6031 \end{bmatrix}y_1 \\ &\quad - \begin{bmatrix} 1.6031 & -1.6031 \end{bmatrix}y_1(0)\exp(-0.015t),\end{aligned} \tag{26}$$

and

$$\begin{aligned}s_2(y_2(t),t) &= \begin{bmatrix} 2.6344 & -2.6344 \end{bmatrix}y_2 \\ &\quad - \begin{bmatrix} 2.6344 & -2.6344 \end{bmatrix}y_2(0)\exp(-0.015t).\end{aligned} \tag{27}$$

The observers (12) take the forms (28) and (29).

$$\dot{\hat{\vartheta}}_1(t)=\begin{bmatrix}\text{-2.1419} & \text{-0.9460}\\ 0.2839 & \text{-0.1081}\end{bmatrix}\hat{\vartheta}_1(t)+\begin{bmatrix}\text{-0.6515}\\ \text{-0.0918}\end{bmatrix}\bar{s}_1(t), \qquad (28)$$

and

$$\dot{\hat{\vartheta}}_2(t)=\begin{bmatrix}\text{-0.7190} & \text{-0.0641}\\ 0.7856 & \text{-0.6810}\end{bmatrix}\hat{\vartheta}_2(t)+\begin{bmatrix}\text{-0.0474}\\ 0.6690\end{bmatrix}\bar{s}_2(t), \qquad (29)$$

where $\bar{s}_1=[1.6031\ \ \text{-1.6031}]y_1$ and $\bar{s}_2=[2.6344\ \ \text{-2.6344}]y_2$.

The estimator error dynamics of the subsystem I and the subsystem II are respectively written as

$$\begin{aligned}\dot{\tilde{\vartheta}}_1(t)&=\begin{bmatrix}\text{-2.350} & \text{-0.729}\\ 0.254 & \text{-0.149}\end{bmatrix}\tilde{\vartheta}_1(t)-\left\{\begin{bmatrix}\text{-0.0249}\\ 0.0499\end{bmatrix}\sin(0.13t)\right.\\ &\left.+\begin{bmatrix}0.0303\\ 0.0607\end{bmatrix}\sin(0.32t)\right\}\bar{s}_1-\begin{bmatrix}\text{-0.208} & 0.216\\ \text{-0.029} & \text{-0.041}\end{bmatrix}\hat{\vartheta}_1-\begin{bmatrix}\text{-0.001}\\ 0.038\end{bmatrix}\bar{s}_1,\end{aligned} \qquad (30)$$

and

$$\begin{aligned}\dot{\tilde{\vartheta}}_2(t)&=\begin{bmatrix}\text{-0.865} & \text{-0.025}\\ 0.667 & \text{-0.684}\end{bmatrix}\tilde{\vartheta}_2(t)-\left\{\begin{bmatrix}\text{-0.033}\\ 0.016\end{bmatrix}\sin(0.11t)\right.\\ &\left.+\begin{bmatrix}0.037\\ \text{-0.074}\end{bmatrix}\sin(0.15t)\right\}\bar{s}_2-\begin{bmatrix}\text{-0.146} & 0.038\\ \text{-0.035} & \text{-0.052}\end{bmatrix}\hat{\vartheta}_2-\begin{bmatrix}0.002\\ 0.063\end{bmatrix}\bar{s}_2.\end{aligned} \qquad (31)$$

Now, by solving LMI (16), it is easy to verify that conditions in Proposition 3.2 are satisfied with positive matrices $\varPsi_1=\begin{bmatrix}0.1380 & -0.0079\\ -0.0079 & 0.3879\end{bmatrix}$ and $\varPsi_2=\begin{bmatrix}3.7788 & 1.6431\\ 1.6431 & 0.9391\end{bmatrix}$. Then, the control signals of two subsystems that produce the chattering phenomenon

$$\begin{aligned}u_{11}(t)=-0.3181s_1-&\Big\{3.046\Big[\big\|\hat{\vartheta}_1(t)\big\|+\tilde{\psi}_1(t)\Big]+3.6062\|y_1\|\\ &+0.001\Big[1.5811\Big(\big\|\hat{\vartheta}_1(t)\big\|+\tilde{\psi}_1(t)\Big)+1.5812\|y_1\|\Big]^2\\ &+\big[0.0149\ \ \text{-0.0149}\big]y_1(0)\exp(\text{-0.0150}t)\Big\}\frac{s_1}{\|s_1\|},\end{aligned} \qquad (32)$$

and

$$\begin{aligned}u_{12}(t)=-0.1936s_2-&\Big\{1.8209\Big[\big\|\hat{\vartheta}_2\big\|+\tilde{\psi}_2(t)\Big]+6.2933\|y_2\|\\ &+0.001\Big[1.5811\Big(\big\|\hat{\vartheta}_2\big\|+\tilde{\psi}_2(t)\Big)+1.5812\|y_2\|\Big]^2\\ &+\big[0.0149\ \ \text{-0.0149}\big]y_2(0)\exp(\text{-0.0150}t)\Big\}\frac{s_2}{\|s_2\|},\end{aligned} \qquad (33)$$

where the upper bound of the observer error $\tilde{\psi}_1(t)$, $\tilde{\psi}_2(t)$ are the solutions of $\dot{\tilde{\psi}}_1(t)=\text{-0.2497}\tilde{\psi}_1(t)+7.2771\times10^{-4}\|\bar{s}_1(t)\|$ and $\dot{\tilde{\psi}}_2(t)=\text{-0.7000}\tilde{\psi}_2(t)+0.65857\times10^{-4}\|\bar{s}_2\|$, respectively.

To solve the chattering in the controllers (32) and (33), we have established the chattering free variable structure controllers for each subsystem as follows

$$\begin{aligned}u_{21}(t)=-\ 0.3181s_1-3.046&\Big[\big\|\hat{\vartheta}_1(t)\big\|+\tilde{\psi}_1(t)\Big]\\ &-0.6238\tilde{\omega}_1(t)\frac{\|\theta_1\|}{\|\theta_1\|+0.001e^{-0.012t}},\end{aligned} \qquad (34)$$

$$\begin{aligned}u_{22}(t)=-\ 0.1936s_2-1.8209&\Big[\big\|\hat{\vartheta}_2(t)\big\|+\tilde{\psi}_2(t)\Big]\\ &-0.3796\tilde{\omega}_2(t)\frac{\|\theta_2\|}{\|\theta_2\|+0.001e^{-0.012t}},\end{aligned} \qquad (35)$$

where $\|\theta_1\|=\tilde{\omega}_1(t)=5.7431\|y_1\|+0{,}016+0.0253(\|\hat{\vartheta}_1\|+\tilde{\psi}_1)$ $+0{,}016[1.5811(\|\hat{\vartheta}_1\|+\tilde{\psi}_1)+1.5812\|y_1\|]^2+[0.0240\ \ \text{-0.0240}]$ $\times y_1(0)\exp(\text{-0.0150}t)$ and $\|\theta_2\|=\tilde{\omega}_2=7.2172\|y_2\|+0{,}0263$ $+0.0416(\|\hat{\vartheta}_2\|+\tilde{\psi}_2)+0{,}0263\,[1.581(\|\hat{\vartheta}_2\|+\tilde{\psi}_2)+1.5812\|y_2\|]^2$ $+[0.0395\ \ \text{-0.0395}]y_2(0)\exp(\text{-0.0150}t)$.

The controllers without the chattering when using the tanh function for two subsystems are calculated as

$$\begin{aligned}u_{31}(t)=-0.3181s_1-&\Big\{3.0460\Big(\big\|\hat{\vartheta}_1\big\|+\tilde{\psi}_1\Big)+3.6062\|y_1\|\\ &+0.001\Big[1.5811\Big(\big\|\hat{\vartheta}_1\big\|+\tilde{\psi}_1\Big)+1.5812\|y_1\|\Big]^2\\ &+\big[0.0149\ \ \text{-0.0149}\big]y_1(0)\exp(\text{-0.0150}t)\Big\}\tanh\left(\frac{s_1}{\|s_1\|}\right),\end{aligned} \qquad (36)$$

and

$$\begin{aligned}u_{32}(t)=-0.1936s_2-&\Big\{1.8209\Big(\big\|\hat{\vartheta}_2\big\|+\tilde{\psi}_2\Big)+6.2933\|y_2\|\\ &+0.001\Big[1.5811\Big(\big\|\hat{\vartheta}_2\big\|+\tilde{\psi}_2\Big)+1.5812\|y_2\|\Big]^2\\ &+\big[0.0149\ \ \text{-0.0149}\big]y_2(0)\exp(\text{-0.0150}t)\Big\}\tanh\left(\frac{s_2}{\|s_2\|}\right).\end{aligned} \qquad (37)$$

The simulation results that show the effectiveness of the proposed controllers are displayed in Figures 6-10.

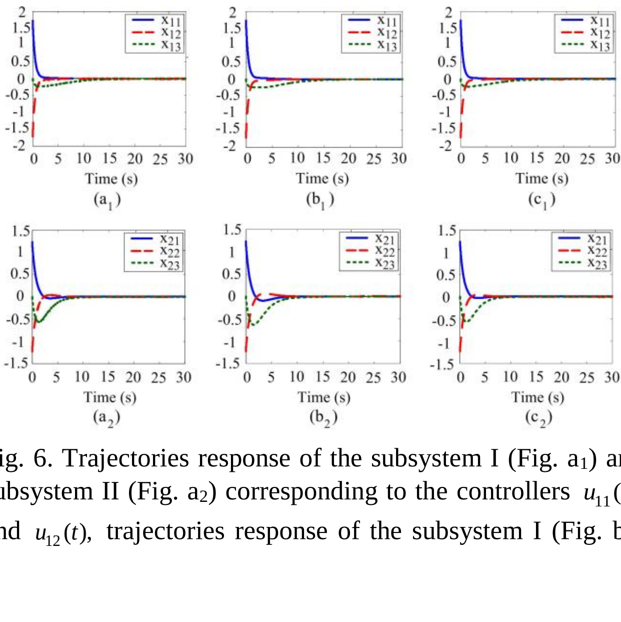

Fig. 6. Trajectories response of the subsystem I (Fig. a1) and subsystem II (Fig. a2) corresponding to the controllers $u_{11}(t)$ and $u_{12}(t)$, trajectories response of the subsystem I (Fig. b1)

and subsystem II (Fig. b2) corresponding to the controllers $u_{21}(t)$ and $u_{22}(t)$, trajectories response of subsystem I (Fig. c1) and subsystem II (Fig. c2) corresponding to controllers $u_{31}(t)$ and $u_{32}(t)$.

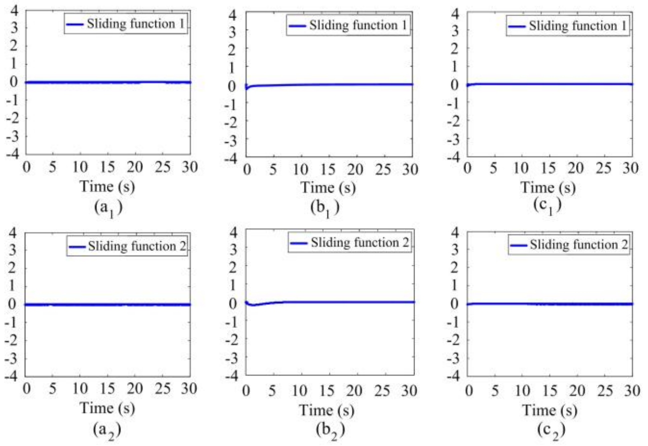

Fig. 7. Time response of the switching functions for each subsystem conforming to the controllers.

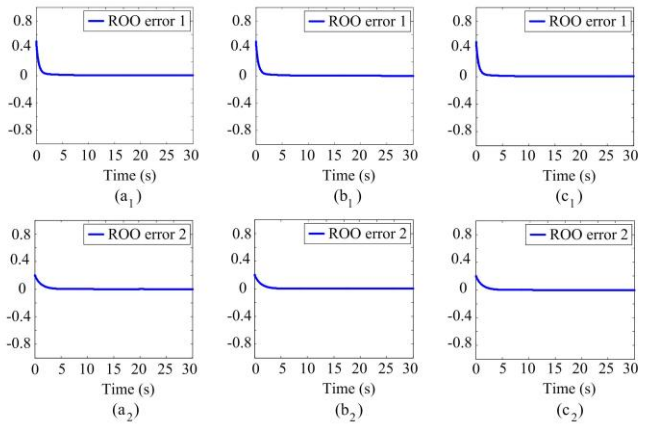

Fig. 8. Time response of the estimator error dynamics for the subsystem I (Fig. 9 a1, b1, c1) and subsystem II (Fig. 9 a2, b2, c2) corresponding to $u_{11}(t)$, $u_{21}(t)$, $u_{31}(t)$ and $u_{12}(t)$, $u_{22}(t)$, $u_{32}(t)$.

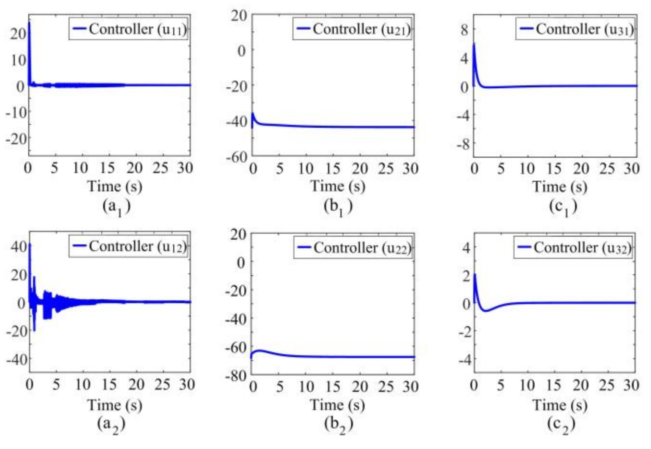

Fig. 9. The amplitude of the control signals $u_{11}(t)$, $u_{21}(t)$, $u_{31}(t)$ and $u_{12}(t)$, $u_{22}(t)$, $u_{32}(t)$ corresponding to the subsystem I and subsystem II.

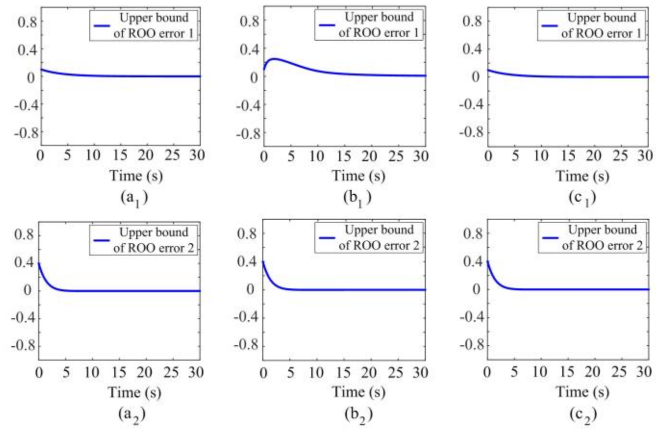

Fig. 10. Time response of the estimator error upper bounds for the subsystem I (Fig. 11 a1, b1, c1) and subsystem II (Fig. 11 a2, b2, c2) corresponding to $u_{11}(t)$, $u_{21}(t)$, $u_{31}(t)$ and $u_{12}(t)$, $u_{22}(t)$, $u_{32}(t)$.

Remark 4.1. The simulation results of the trajectories states for the subsystem I and subsystem II are shown in Fig. 7 (a1, b1, c1) and Fig. 7 (a2, b2, c2), respectively. One can see that the state responses of each subsystem asymptotically approach to zero and stay at it for the subsequent time. In details, Fig. 7 a1 and Fig. 7 a2 are results of the controlled systems by using $u_{11}(t)$ and $u_{12}(t)$ that occur the chattering phenomenon, respectively. To solve this undesired chattering, the two solutions containing the well-known Barbalat lemma with the controllers $u_{21}(t)$, $u_{22}(t)$ and the tanh function with the controllers $u_{31}(t)$, $u_{32}(t)$ are used in this paper. Fig. 7 b1 and Fig. 7 b2 are the trajectories states of the subsystems when utilize the Barbalat lemma and the time response reaches to zero after about 10 seconds. Fig. 7 c1 and Fig. 7 c2 are the trajectories states of each subsystem when use the tanh function and the response time drives to zero after about 6.0 seconds. As a result, it is clearly that the controlled states that use the tanh function converge faster and these figures display the asymptotic stability of the subsystems despite the existence of external perturbations. In other words, by using the proposed controllers from (32) to (37), the trajectories of the subsystems reach the switching surface $s_i(y_i(t),t)=0$ from the instance time $(t \geq 0)$ where the recent researches (Gao et al., 2019; Huynh et al., 2018; Li and Zhang, 2019; Ranjbar et al., 2020) could not obtain the attainment.

Remark 4.2. The time response for each subsystem that governed by the switching functions (26) and (27) are shown in Fig. 8. a1, b1, c1 (for subsystem I) and Fig. 8. a2, b2, c2 (for subsystem II), respectively. It is obvious that the sliding variables of each subsystem approaches zero from the beginning time $(t \geq 0)$ which is signified the elimination of the reaching phase in the CVSC. That is, the trajectories states of the subsystems always start from the switching surface and the desired response of the plant is ensured from the commencing of its motion. Therefore, the robustness and performance of the whole system have been enhanced. Compared with the previous works (Al-khazraji et al., 2011) which only applied to the small systems, this is one of the key achievements of our study for the complex interconnected systems.

Remark 4.3. Fig. 9 depicts the time behaviour of the ROO's error convergence, $\tilde{\vartheta}_i(t) = \hat{\vartheta}_i(t) - \vartheta_i(t)$, between the actual and that of the estimated state for each subsystem. The response time of the observer error dynamics of the subsystems rapidly convergent to zero. In addition, the ROO error is bounded by the upper bound $\tilde{\psi}_i(t)$ (15), whose dynamics response is exhibited in Fig. 11. It shows that the proposed ROO can be used to reconstruct the unmeasurable state variables of the systems (1) and the response time of the resultant closed-loop system is asymptotically driven to zero. Besides, the proposed ROO has been designed based on the conventional Luenberger observer (Luenberger, 1971). The parameters of the ROO have been selected to ensure the invariance property. Compared with the FOO in (Koo et al., 2014; Li and Zhang, 2019), which increase the complexity of the design and computation load. Therefore, the novel ROO with the lower-dimensional solution in this paper has been solved these drawbacks.

Remark 4.4. The control signal responses of the subsystem I and subsystem II are exposed in Fig. 10. Fig. 10 a_1 and Fig. 10 b_1 respectively are the results of the controllers $u_{11}(t)$ (32) and $u_{12}(t)$ (33) that cause the unwanted chattering phenomenon. Fig. 10 b_1, b_2 and Fig. 10 c_1, c_2 are the responses of the chattering suppression controllers $u_{21}(t)$ (34) , $u_{22}(t)$ (35) and $u_{31}(t)$ (36), $u_{32}(t)$ (37) which respectively use the Barbalat lemma and the tanh function. It is obviously seen that the violent chattering effect is alleviated as well as the state trajectory of the subsystems approaches to zero. Comparing with Fig. 10 b_1, b_2, the magnitude of the control signal that displayed in Fig. 10 c_1, c_2 is quite small and the state trajectories of the subsystems is driven into the sliding surface in finite time. It is needed to tackle the external disturbances or the effects of the uncertainties and interconnections before the system enters the sliding mode. This technique gives better performance than the other approaches published in (Gao et al., 2019; Yang et al., 2015). Concurrently, the limitations of VSC approaches for linear systems with unknown interconnections in the latest paper (Ranjbar et al., 2020) have been removed.

From above simulation results, we can conclude that the proposed technique is efficient for solving the undesired chattering phenomenon and stabilize the mismatched uncertain interconnected systems even at the existence of the extended disturbances.

5. CONCLUSIONS

In this paper, a chattering suppression single phase variable structure controller (CSSPVSC) has been proposed to stabilize and alleviate the undesired high frequency oscillation in control signal for mismatched uncertain interconnected systems with external disturbances. In the CSSPVSC, we have investigated the output feedback and estimated state variables only. Furthermore, in these systems, the exogenous perturbations which effect on the systems have been extended to the polynomial function of the state variables. By combining a Moore-Penrose Inverse approach and the tanh function, the restrictions in the recent publication (Ranjbar et al., 2020) have been removed. In addition, the sufficient condition in the LMI format employing the Lyapunov functional has been derived to guarantee the asymptotic stability of the closed-loop system. At last, the example is provided to demonstrate the effectiveness and merits of the proposed technique. Hence, the application of the presented approach to the practical control systems such as power converters, electrical drives, and mobile robots in continuous time domain could be the future goal.

ACKNOWLEDGMENT

The authors wish to express their gratitude to Van Lang University, Vietnam for financial support for this research.

NOMENCLATURE

A^{-1}	inverse of A matrix
A^T	transpose of A matrix
$B^{\perp}$	perpendicular complement of B matrix
E^g	Moore-Penrose inverse of E matrix
$f(x, t)$	disturbance input
$s(y(t), t)$	sliding surface
$u(t)$	control signal
$x(t)$	states of the system
$\lVert x(t) \rVert$	norm of the state vector $x(t)$
$y(t)$	output signal
$\lambda_{\max}$	maximum eigenvalue
Ψ	positive matrix
$\tilde{\varpi}$, φ, $\tilde{\gamma}$,	positive constants

REFERENCES

Al-khazraji, A., Essounbouli, N., Hamzaoui, A., Nollet, F., and Zaytoon, J. (2011). Type-2 fuzzy sliding mode control without reaching phase for nonlinear system. *Engineering Applications using Artificial Intelligence*, vol. 24, no. 1, pp. 23–38.

Boiko, I. M. (2011). Chattering in sliding mode control systems with boundary layer approximation of discontinuous control. *International Journal of Systems Science*, vol. 44, no. 6, pp. 1126–1133.

Boyd, S., El Ghaoui, L., Feron, E., and Balakrishnan, V. (1994). *Linear Matrix Inequalities in System and Control Theory*. Society for Industrial and Applied Mathematics (SIAM), Philadelphia, pa, USA.

Cheng, C. C., and Chang, Y. (2008). Design of decentralised adaptive sliding mode controllers for large-scale systems with mismatched perturbations. *International Journal of Control*, vol. 81, no. 10, pp. 1507–1518.

Choi, H. H. (2007). Frequency domain interpretations of the invariance condition of sliding mode control theory. *IET Control Theory and Applications,* vol. 1, no. 4, pp. 869–874.

Chung, C. -W., and Chang, Y. (2011). Design of a sliding mode controller for decentralised multi-input systems. *IET Control Theory and Applications,* vol. 5, no. 1, pp. 221–230.

Gahinet, P., Nemirovskii, A., Laub, A. J., and Chilali, M. (1994). *LMI Control Toolbox*. Natick, MA: The MathWorks, Inc.

Gao, R., Zhang, Q., and Li, J. (2019). Integral sliding mode control for interconnected descriptor systems based on a reduced-order observer. *International Journal of Systems Science*, vol. 50, no. 10, pp. 1947–1960.

Ghasemi, R., Menhaj, M. B., and Afshar, A. (2009). A new decentralized fuzzy model reference adaptive controller for a class of large-scale non-affine nonlinear systems. *European Journal of Control,* vol. 15, no. 5, pp. 534–545.

Gopalsamy, K. (1992). *Stability and Oscillations in Delay Differential Equations of Population Dynamics*. Dordrecht, The Netherlands: Kluwer.

Huynh, V. V., Vo, H. D., Dinh, B. H., Tran, T. P., and Tran, M. H. Q. (2018). A new adaptive second order sliding mode control design for complex interconnected systems. *Journal of Control Engineering and Applied Informatics,* vol. 20, no. 1, pp. 3–14.

Koo, G. B., Park, J. B., and Joo, Y. H. (2014). Decentralized fuzzy observerbased output-feedback control for nonlinear large-scale systems: An LMI approach. *IEEE Transactions on Fuzzy Systems,* vol. 22, no. 2, pp. 406–419.

Li, J., and Zhang, Q. (2019). Fuzzy reduced-order compensator-based stabilization for interconnected descriptor systems via integral sliding modes. *IEEE Transactions on Systems, Man, and Cybernetics: Systems*, vol. 49, no. 4, pp. 752–765.

Lian, J., and Zhao, J. (2009). Output feedback variable structure control for a class of uncertain switched systems. *Asian Journal of Control,* vol. 11, no. 1, pp. 1–9.

Luenberger, D. (1971). An introduction to observers. *IEEE Transactions Automatic Control,* vol. 16, no. 6, pp. 596–602.

Mantz, R. J., De Battista, H., and Puleston, P. F. (2001). A new approach to reaching mode of VSS using trajectory planning. *Automatica,* vol. 37, no. 5, pp. 763–767.

Mondal, S., and Mahanta, C. (2013). Adaptive integral higher order sliding mode controller for uncertain systems. *Journal of Control Theory and Application,* vol. 11, no. 1, pp. 61–68.

Nguyen, C. T., and Tsai, Y.-W. (2017). Finite-time output feedback controller based on observer for the time-varying delayed systems: A Moore-Penrose Inverse approach. *Mathematical Problems in Engineering,* vol. 2017, pp. Article ID 2808094, 2808013 pages.

Ranjbar, B., Ranjbar Noiey, A., and Rezaie, B. (2020). Adaptive sliding mode observer based decentralized control design for linear systems with unknown interconnections. *Journal of Vibration and Control*. doi: 10.1177/1077546320925359

Salem, F. B., Bahri, I., Maamri, H., and Derbel, N. (2020). A second-order sliding mode control of switched reluctance motor. *Electric Power Components and Systems*, vol. 48, no. 6-7, pp. 640–651.

Shi, S.-L., Li, J.-X., and Fang, Y.-M. (2018). Extended-state-observer-based chattering free sliding mode control for nonlinear systems with mismatched disturbance. *IEEE Access,* vol. 6, pp. 22952–22957.

Shyu, K. -K., Tsai, Y.-W., Yu, Y., and Lai, C.-K. (2000). Decentralized dynamic output feedback controllers for interconnected systems with mismatched uncertainties using new sliding mode control. *International Journal of Systems Science,* vol. 31, no. 8, pp. 1011–1020.

Shyu, K. -K., Tsai, Y. -W., and Lai, C. -K. (2001). A dynamic output feedback controller for mismatched uncertain variable systems. *Automatica,* vol. 37, pp. 775–779.

Soltanpour, M. R., Zaare, S., Haghgoo, M., and Moattari, M. (2020). Free-chattering fuzzy sliding mode control of robot manipulators with joints flexibility in presence of matched and mismatched uncertainties in model dynamic and actuators. *Journal of Intelligent & Robotic Systems,* vol. 100, no. 1, pp. 47–69.

Xue, Y. M., Zheng, B. C., and Ye, D. (2015). Quantized feedback control design of nonlinear large-scale systems via decentralized adaptive integral sliding mode control. *Mathematical Problems in Engineering,* vol. 2015, Article ID 718924, 12 pages.

Yan, X. G., Spurgeon, S. K., and Edwards, C. (2012). Global decentralised static output feedback sliding mode control for interconnected time-delay systems. *IET Control Theory and Applications,* vol. 6, no. 2, pp. 192–202.

Yang, Y., Yue, D., and Xue, Y. S. (2015). Decentralized adaptive neural output feedback control of a class of large- scale time-delay systems with input saturation. *Journal of The Franklin Institute,* vol. 352, no. 5, pp. 2129–2151.

Zhang, J., and Xia, Y. (2010). Design of static output feedback sliding mode control for uncertain linear systems. *IEEE Transactions on Industrial Electronics,* vol. 57, no. 6, pp. 2161–2170.

Zhang, T. P., and Mei, J. D. (2006). Decentralized direct adaptive neural network control for a class of interconnected systems. *Journal of Systems Engineering and Electronics,* vol. 17, no. 2, pp. 374–380.

Zhang, T. P., Zhou, C. Y., and Zhu, Q. (2009). Adaptive variable structure control of MIMO nonlinear systems with time-varying delays and unknown dead-zones. *International Journal of Automation and Computing,* vol. 6, no. 2, pp. 124–136.

Zheng, B. C., and Yang, G. H. (2013). Decentralized sliding mode quantized feedback control for a class of uncertain large-scale systems with dead-zone input nonlinearities. *Journal of Nonlinear Dynamics,* vol. 71, no. 3, pp. 417–427.

APPENDIXES

Appendix A: Proof of Proposition 3.1

The matrix $\bar{A}_{ii11}$ of system (14) being stable, we have $\left\|\exp(\bar{A}_{ii11}t)\right\| \le \tilde{\varepsilon}_i \exp(\lambda_{\max_i} t)$ for some constants $\tilde{\varepsilon}_i$. Then, after calculating the norms of both sides of (14), using the triangle inequality for the right side, and multiplying the resulting inequality with $\exp(-\lambda_{\max_i} t)$, follows:

$$\begin{aligned}
&\left\|\tilde{\vartheta}_i(t)\right\|\exp(-\lambda_{\max_i}t) \\
&\le \tilde{\varepsilon}_i\left\|\tilde{\vartheta}_i(0)\right\| + \int_0^t \tilde{\varepsilon}_i \exp(-\lambda_{\max_i}\tau)\sum_{j=1, j\ne i}^{L}\left[\left\|\bar{K}_{ji11}\right\|\left\|\tilde{\vartheta}_i(\tau)\right\|\right]d\tau \\
&+ \int_0^t \tilde{\varepsilon}_i \exp(-\lambda_{\max_i}\tau)\times\left\{\left\|B_i^{\perp T}D_{ii}\right\|\left\|E_{ii}B_i\left(T_iB_i\right)^{-1}\right\|\left\|\bar{s}_i(\tau)\right\|\right. \qquad (38)\\
&+ \sum_{j=1, j\ne i}^{L}\left[\left\|\bar{K}_{ji11}\right\|\left\|\hat{\vartheta}_i(\tau)\right\| + \left\|\bar{K}_{ji12}\right\|\left\|\bar{s}_i(\tau)\right\|\right] \\
&\left.+ \sum_{j=1, j\ne i}^{L}\left[\left\|B_j^{\perp T}G_{ji}\right\|\left\|H_{ji}B_j\left(T_jB_j\right)^{-1}\right\|\left\|\bar{s}_i(\tau)\right\|\right]\right\}d\tau.
\end{aligned}$$

In order to determine the upper bound of estimation error, we recall the following lemma.

Lemma 1. (Shyu et al., 2001) Assume $C' \ge 0,\ r(t),\ h(t),$ and $g(t)$ are non-negative valued continuous functions of time. If $r(t) \le C' + \int_{t_0}^{t} h(\tau)r(\tau)d\tau + \int_{t_0}^{t} g(\tau)d\tau,$ then $r(t) \le C'\exp\{f(t)\}$ $+\int_{t_0}^{t} g(\tau)\exp\{f(t)-f(\tau)\}d\tau,$ where $f(t) = \int_{t_0}^{t} h(\tau)d\tau.$

Now, by applying the Lemma 1 above, we symbolize

$$\begin{aligned}
&r(t) = \left\|\tilde{\vartheta}_i\right\|\exp(-\lambda_{\max_i}t),\ C' = \tilde{\varepsilon}_i\left\|\tilde{\vartheta}_i(0)\right\|,\ h = \tilde{\varepsilon}_i\sum_{j=1, j\ne i}^{L}(\left\|\bar{K}_{ji11}\right\|),\\
&g(t) \ = \ \tilde{\varepsilon}_i\exp(-\lambda_{\max_i}t)\left\{\left\|B_i^{\perp T}D_{ii}\right\|\left\|E_{ii}B_i\left(T_iB_i\right)^{-1}\right\|\left\|\bar{s}_i(t)\right\|\right.\\
&+\sum_{\substack{j=1\\ j\ne i}}^{L}\left[\left\|\bar{K}_{ji11}\right\|\left\|\hat{\vartheta}_i\right\| + \left\|\bar{K}_{ji12}\right\|\left\|\bar{s}_i\right\|\right] + \sum_{j=1, j\ne i}^{L}\left[\left\|B_j^{\perp T}G_{ji}\right\|\left\|H_{ji}B_j\left(T_jB_j\right)^{-1}\right\|\right.\\
&\left.\left.\times\left\|\bar{s}_i(t)\right\|\right]\right\},\ f(t) = \int_0^t h(\tau)d\tau = \tilde{\varepsilon}_i\sum_{j=1, j\ne i}^{L}\left(\left\|\bar{K}_{ji11}\right\|\right)t.
\end{aligned}$$

We obtain

$$\begin{aligned}
&\left\|\tilde{\vartheta}_i(t)\right\|\exp(-\lambda_{\max_i}t) \le \tilde{\varepsilon}_i\left\|\tilde{\vartheta}_i(0)\right\|\exp\left(\tilde{\varepsilon}_i\sum_{j=1, j\ne i}^{L}\left(\left\|\bar{K}_{ji11}\right\|\right)t\right)\\
&+\int_0^t \tilde{\varepsilon}_i\exp(-\lambda_{\max_i}\tau)\left\{\left\|B_i^{\perp T}D_{ii}\right\|\left\|E_{ii}B_i\left(T_iB_i\right)^{-1}\right\|\left\|\bar{s}_i(\tau)\right\|\right.\\
&+\sum_{j=1, j\ne i}^{L}\left[\left\|\bar{K}_{ji11}\right\|\left\|\hat{\vartheta}_i(\tau)\right\| + \left\|\bar{K}_{ji12}\right\|\left\|\bar{s}_i(\tau)\right\|\right]\\
&\left.+\sum_{j=1, j\ne i}^{L}\left[\left\|B_j^{\perp T}G_{ji}\right\|\left\|H_{ji}B_j\left(T_jB_j\right)^{-1}\right\|\left\|\bar{s}_i(\tau)\right\|\right]\right\} \qquad (39)\\
&\times\exp\left(\tilde{\varepsilon}_i\sum_{j=1, j\ne i}^{L}\left(\left\|\bar{K}_{ji11}\right\|\right)\tau - \tilde{\varepsilon}_i\sum_{\substack{j=1\\ j\ne i}}^{L}\left(\left\|\bar{K}_{ji11}\right\|\right)\tau\right)d\tau.
\end{aligned}$$

The above inequality (39) can be rewritten as

$$\begin{aligned}
&\left\|\tilde{\vartheta}_i(t)\right\|\\
&\le \tilde{\varepsilon}_i\left\|\tilde{\vartheta}_i(0)\right\|\exp\left[\left(\lambda_{\max_i} + \tilde{\varepsilon}_i\sum_{\substack{j=1\\ j\ne i}}^{L}\left\|\bar{K}_{ji11}\right\|\right)t\right] + \int_0^t \tilde{\varepsilon}_i\exp\left[\left(\lambda_{\max_i}\right.\right.\\
&\left.\left.+\tilde{\varepsilon}_i\sum_{\substack{j=1\\ j\ne i}}^{L}\left\|\bar{K}_{ji11}\right\|\right)(t-\tau)\right]\left\{\left\|B_i^{\perp T}D_{ii}\right\|\left\|E_{ii}B_i\left(T_iB_i\right)^{-1}\right\|\left\|\bar{s}_i(\tau)\right\|\right.\\
&+\sum_{\substack{j=1\\ j\ne i}}^{L}\left[\left\|\bar{K}_{ji11}\right\|\left\|\hat{\vartheta}_i(\tau)\right\| + \left\|\bar{K}_{ji12}\right\|\left\|\bar{s}_i(\tau)\right\|\right]\\
&\left.+\sum_{\substack{j=1\\ j\ne i}}^{L}\left[\left\|B_j^{\perp T}G_{ji}\right\|\left\|H_{ji}B_j\left(T_jB_j\right)^{-1}\right\|\left\|\bar{s}_i(\tau)\right\|\right]\right\}d\tau,\\
&\le \tilde{\psi}_i(0)\exp\left[\left(\lambda_{\max_i} + \tilde{\varepsilon}_i\sum_{j=1, j\ne i}^{L}\left\|\bar{K}_{ji11}\right\|\right)t\right] + \int_0^t \tilde{\varepsilon}_i\exp\left[\left(\lambda_{\max_i}\right.\right.\\
&\left.\left.+\tilde{\varepsilon}_i\sum_{j=1, j\ne i}^{L}\left\|\bar{K}_{ji11}\right\|\right)(t-\tau)\right]\left\{\left\|B_i^{\perp T}D_{ii}\right\|\left\|E_{ii}B_i\left(T_iB_i\right)^{-1}\right\|\right.\\
&+\sum_{j=1, j\ne i}^{L}\left[\left\|B_j^{\perp T}G_{ji}\right\|\left\|H_{ji}B_j\left(T_jB_j\right)^{-1}\right\|\right]\left\|\bar{s}_i(\tau)\right\|\\
&\left.+\sum_{j=1, j\ne i}^{L}\left[\left\|\bar{K}_{ji11}\right\|\left\|\hat{\vartheta}_i(\tau)\right\| + \left\|\bar{K}_{ji12}\right\|\left\|\bar{s}_i(\tau)\right\|\right]\right\}d\tau
\end{aligned}$$

$= \tilde{\psi}_i(t),$ where $\tilde{\psi}_i(t)$ satisfies (15). Thus, we can conclude that $\left\|\tilde{\vartheta}_i(t)\right\| \le \tilde{\Psi}_i(t)$ for all time. The proof of Proposition 3.1 is completed. □

Appendix B: Proof of Proposition 3.2

The first equation (8) can be described in the sliding mode, $\bar{s}_i(t) = 0,$ as follows:

$$\dot{\vartheta}_i(t) = \left[\bar{A}_{ii11} + \tilde{D}_{ii}\Sigma_{ii}\tilde{E}_{ii}\right]\vartheta_i + \sum_{j=1, j\ne i}^{L}\left\{\left[\bar{K}_{ji11} + \tilde{G}_{ji}\Sigma_{ji}\tilde{H}_{ji}\right]\vartheta_i\right\}. \qquad (40)$$

Now, we have selected the Lyapunov function candidate as $V_B = \sum_{i=1}^{L}\vartheta_i^T(t)\Psi_i\vartheta_i(t).$ Then, by using (40), the time derivative of V_B is given by

$$\begin{aligned}
\dot{V}_B &= \sum_{i=1}^{L}\vartheta_i^T(t)\left[\bar{A}_{ii11}^T\Psi_i + \Psi_i\bar{A}_{ii11} + \Psi_i\tilde{D}_{ii}\Sigma_{ii}(x_i,t)\tilde{E}_{ii}\right.\\
&\left.+\tilde{E}_{ii}^T\Sigma_{ii}^T(x_i,t)\tilde{D}_{ii}^T\Psi_i\right]\vartheta_i(t) + \sum_{i=1}^{L}\sum_{j=1, j\ne i}^{L}\vartheta_i^T(t)\left[\bar{K}_{ji11}^T\Psi_i\right. \qquad (41)\\
&\left.+\Psi_i\bar{K}_{ji11} + \Psi_i\tilde{G}_{ji}\Sigma_{ji}(x_j,t)\tilde{H}_{ji} + \tilde{H}_{ji}^T\Sigma_{ji}^T(x_j,t)\tilde{G}_{ji}^T\Psi_i\right]\vartheta_i.
\end{aligned}$$

Applying the Lemma 1 published in (J. Zhang and Xia, 2010) to equation (41), we get

$$\begin{aligned}
\dot{V}_B &\le \sum_{i=1}^{L}\vartheta_i^T(t)\left[\bar{A}_{ii11}^T\Psi_i + \Psi_i\bar{A}_{ii11} + \varphi_i^{-1}\Psi_i\tilde{D}_{ii}\tilde{D}_{ii}^T\Psi_i + \varphi_i\tilde{E}_{ii}^T\tilde{E}_{ii}\right.\\
&\left.+\sum_{j=1, j\ne i}^{L}\left(\bar{K}_{ji11}^T\Psi_i + \Psi_i\bar{K}_{ji11} + \varphi_j^{-1}\Psi_i\tilde{G}_{ji}\tilde{G}_{ji}^T\Psi_i + \varphi_j\tilde{H}_{ji}^T\tilde{H}_{ji}\right)\right]\vartheta_i, \qquad (42)
\end{aligned}$$

where φ_i and φ_j are positive scalars.

By utilizing Lemma 2 in (Huynh et al., 2018), the above equation can be rewritten as

$$\dot{V}_B \le \sum_{i=1}^{L} \vartheta_i^T \Big(\bar{A}_{ii11}^T \varPsi_i + \varPsi_i \bar{A}_{ii11} + \varphi_i^{-1} \varPsi_i \tilde{D}_{ii} \tilde{D}_{ii}^T \varPsi_i + \varphi_i \tilde{E}_{ii}^T \tilde{E}_{ii} + \frac{L-1}{\tilde{\gamma}_i} \times \varPsi_i \varPsi_i + \sum_{j=1, j\ne i}^{L} \Big(\tilde{\gamma}_j \bar{K}_{ji11}^T \bar{K}_{ji11} + \varphi_i^{-1} \varPsi_i \tilde{G}_{ji} \tilde{G}_{ji}^T \varPsi_i + \varphi_i \tilde{H}_{ji}^T \tilde{H}_{ji} \Big) \Big) \vartheta_i, \quad (43)$$

where $\tilde{\gamma}_i$, $\tilde{\gamma}_j$ are positive scalars.

Now, by applying the Schur complement (Boyd et al., 1994) to the LMI equation (16), we have

$$\bar{A}_{ii11}^T \varPsi_i + \varPsi_i \bar{A}_{ii11} + \sum_{j=1, j\ne i}^{L} \Big(\tilde{\gamma}_j \bar{K}_{ji11}^T \bar{K}_{ji11} + \varphi_i^{-1} \varPsi_i \tilde{G}_{ji} \tilde{G}_{ji}^T \varPsi_i + \varphi_i \tilde{H}_{ji}^T \tilde{H}_{ji} \Big) + \varphi_i^{-1} \varPsi_i \tilde{D}_{ii} \tilde{D}_{ii}^T \varPsi_i + \varphi_i \tilde{E}_{ii}^T \tilde{E}_{ii} + \frac{L-1}{\tilde{\gamma}_i} \varPsi_i \varPsi_i < 0. \quad (44)$$

Combining the equations (43) and (44), it is easy to achieve that $\dot{V}_B < 0$. This inequality shows that if LMI (16) is feasible, then the interconnected systems (1) is asymptotically stable in the sliding mode. □

Appendix C: Proof of Proposition 3.3

Let us consider the Lyapunov function candidate $V_C = \sum_{i=1}^{L} \|s_i\|$, where s_i is the switching function as the equation (3) and use the property

$$\sum_{j=1, j\ne i}^{L} \Big\{ \big[\bar{K}_{ij21} + \Delta \bar{K}_{ij21d_j} \big] \vartheta_j(t) + \big[\bar{K}_{ij22} + \Delta \bar{K}_{ij22} \big] \bar{s}_j(t) \Big\} = \sum_{j=1, j\ne i}^{L} \Big\{ \big[\bar{K}_{ji21} + \Delta \bar{K}_{ji21} \big] \vartheta_i(t) + \big[\bar{K}_{ji22} + \Delta \bar{K}_{ji22} \big] \bar{s}_i(t) \Big\}.$$

Then, the time derivative of V_C is achieved as

$$\dot{V}_C = \sum_{i=1}^{L} \frac{s_i^T}{\|s_i\|} \Big\{ \big[\bar{A}_{ii21} + \Delta \bar{A}_{ii21} \big] \vartheta_i(t) + \big[\bar{A}_{ii22} + \Delta \bar{A}_{ii22} \big] \bar{s}_i(t) + (S_i B_i) \big[u_i(t) + f_i(x_i, t) \big] + \sum_{j=1, j\ne i}^{L} \Big[\big(\bar{K}_{ji21} + \Delta \bar{K}_{ji21} \big) \vartheta_i + \big(\bar{K}_{ji22} + \Delta \bar{K}_{ji22} \big) \bar{s}_i(t) \Big] + \alpha_i F_i y_i(0) \exp(-\alpha_i t) \Big\}. \quad (45)$$

Because $\|\vartheta_i(t)\| \le \|\hat{\vartheta}_i(t)\| + \|\tilde{\vartheta}_i(t)\|$ and $\|\tilde{\vartheta}_i(t)\| \le \tilde{\psi}_i(t)$ that shown in above Proposition 3.1. Based on the state transformation $\bar{M}_i$ in (7), we have

$$\|x_i\| \le \Big\| Q_i B_i^{\perp} \big(B_i^{\perp T} Q_i B_i^{\perp} \big)^{-1} \Big\| \Big[\|\hat{\vartheta}_i\| + \tilde{\psi}_i \Big] + \Big\| B_i (T_i B_i)^{-1} \Big\| \|\bar{s}_i\|. \quad (46)$$

From the equations (46) and (9), the equation (45) can be represented as

$$\dot{V}_C \le \sum_{i=1}^{L} \Big\{ \Big(\|\bar{A}_{ii21}\| + \|R_i B_i^T Q_i^{-1} D_{ii}\| \Big\| E_{ii} Q_i B_i^{\perp} \big(B_i^{\perp T} Q_i B_i^{\perp} \big)^{-1} \Big\| \Big) \times \Big(\|\hat{\vartheta}_i(t)\| + \tilde{\psi}_i(t) \Big) + \sum_{j=1, j\ne i}^{L} \Big[\|\bar{K}_{ji21}\| + \|T_j G_{ji}\| \Big\| H_{ji} Q_j B_j^{\perp} \times \big(B_j^{\perp T} Q_j B_j^{\perp} \big)^{-1} \Big\| \Big] \Big(\|\hat{\vartheta}_i(t)\| + \tilde{\psi}_i(t) \Big) + \sum_{j=1, j\ne i}^{L} \Big(\|\bar{K}_{ji22}\| + \|T_j G_{ji}\| \Big\| H_{ji} B_j (T_j B_j)^{-1} \Big\| \Big) \|F_i\| \|y_i\| + \Big(\|\bar{A}_{ii22}\| + \|R_i B_i^T Q_i^{-1} D_{ii}\| \Big\| E_{ii} B_i (T_i B_i)^{-1} \Big\| \Big) \|F_i\| \|y_i\| + \|(T_i B_i)\| \|f_i\| + \alpha_i F_i y_i(0) \exp(-\alpha_i t) + \frac{s_i^T}{\|s_i\|} (T_i B_i) u_i(t) \Big\}, \quad (47)$$

where $\|f_i\|$ is defined in the equation (17).

By replacing the control signal (17) into (47), we find $\dot{V}_C < 0$, and consequently, the system (1) is lead to the switching surface from zero reaching time. □

Appendix D: Proof of Proposition 3.4

The control signal is almost usually investigated by using Lyapunov function. Let us define the Lyapunov's function as $V_D = \sum_{i=1}^{L} \|s_i\|$. After differentiating V_D with respect to time this yields

$$\dot{V}_D = \sum_{i=1}^{L} \frac{s_i^T}{\|s_i\|} \Big\{ \Big(\bar{A}_{ii21} + R_i B_i^T Q_i^{-1} D_{ii} \varSigma_{ii} E_{ii} Q_i B_i^{\perp} \big(B_i^{\perp T} Q_i B_i^{\perp} \big)^{-1} \Big) \vartheta_i + \Big(\bar{A}_{ii22} + R_i B_i^T Q_i^{-1} D_{ii} \varSigma_{ii} E_{ii} B_i (T_i B_i)^{-1} \Big) \bar{s}_i + (T_i B_i) u_i + (T_i B_i) f_i + \sum_{j=1, j\ne i}^{L} \Big[\Big(\bar{K}_{ji21} + T_j G_{ji} \varSigma_{ji} H_{ji} Q_j B_j^{\perp} \big(B_j^{\perp T} Q_j B_j^{\perp} \big)^{-1} \Big] \vartheta_i + \Big(\bar{K}_{ji22} + T_j G_{ji} \varSigma_{ji} H_{ji} B_j (T_j B_j)^{-1} \Big) \bar{s}_i \Big] + \alpha_i F_i y_i(0) \exp(-\alpha_i t) \Big\}. \quad (48)$$

From the equation (48) and property $\|AB\| \le \|A\| \|B\|$, it creates

$$\dot{V}_D \le \sum_{i=1}^{L} \Big\{ \Big(\|\bar{A}_{ii21}\| + \|R_i B_i^T Q_i^{-1} D_{ii}\| \Big\| E_{ii} Q_i B_i^{\perp} \big(B_i^{\perp T} Q_i B_i^{\perp} \big)^{-1} \Big\| \Big) \times \Big[\|\hat{\vartheta}_i(t)\| + \tilde{\psi}_i(t) \Big] + \sum_{j=1, j\ne i}^{L} \Big(\|\bar{K}_{ji21}\| + \|T_j G_{ji}\| \Big\| H_{ji} Q_j B_j^{\perp} \times \big(B_j^{\perp T} Q_j B_j^{\perp} \big)^{-1} \Big\| \Big) \Big[\|\hat{\vartheta}_i\| + \tilde{\psi}_i \Big] + \sum_{j=1, j\ne i}^{L} \Big(\|\bar{K}_{ji22}\| + \|T_j G_{ji}\| \times \Big\| H_{ji} B_j (T_j B_j)^{-1} \Big\| \Big) \|F_i\| \|y_i\| + \Big(\|\bar{A}_{ii22}\| + \|R_i B_i^T Q_i^{-1} D_{ii}\| \times \Big\| E_{ii} B_i (T_i B_i)^{-1} \Big\| \Big) \|F_i\| \|y_i\| + \|(T_i B_i)\| \sum_{k=0}^{r} \Big[\big(\tilde{\varpi}_{2_i} \big)_k \times \Big\| Q_i B_i^{\perp} \big(B_i^{\perp T} Q_i B_i^{\perp} \big)^{-1} \Big\| \Big[\|\hat{\vartheta}_i(t)\| + \tilde{\psi}_i(t) \Big] + \Big\| B_i (T_i B_i)^{-1} \Big\| \times \|F\|_i \|y_i\| \Big)^k \Big] + \alpha_i \|F_i\| \|y_i(0)\| \exp(-\alpha_i t) + \frac{s_i^T}{\|s_i\|} (T_i B_i) u_i \Big\}. \quad (49)$$

Substituting the control signal (19) into the equation (49), we get

$$\dot{V}_D \le \sum_{i=1}^{L} \tilde{\omega}_i(t) - \sum_{i=1}^{L} \bar{\alpha}_i \|s_i\| - \sum_{i=1}^{L} \frac{\theta_i^T \theta_i}{\|\theta_i\| + \hat{\eta}_i e^{-\gamma_i t}}. \qquad (50)$$

It is noted that $\|\theta_i\| = \tilde{\omega}_i(t)$ and $\|\theta_i\|^2 = \theta_i^T \theta_i$. Hence

$$\dot{V}_D \le -\sum_{i=1}^{L} \bar{\alpha}_i \|s_i\| + \sum_{i=1}^{L} \left[\tilde{\omega}_i(t) - \frac{\theta_i^T \theta_i}{\|\theta_i\| + \hat{\eta}_i e^{-\gamma_i t}} \right],$$

$$\le -\sum_{i=1}^{L} \bar{\alpha}_i \|s_i\| + \sum_{i=1}^{L} \left(\frac{\tilde{\omega}_i(t) \hat{\eta}_i e^{-\gamma_i t}}{\|\theta_i\| + \hat{\eta}_i e^{-\gamma_i t}} \right). \qquad (51)$$

Applying the formula $0 \le ab/(a+b) \le a,\ \forall a, b \ge 0$, we achieve $\dot{V}_D \le -\sum_{i=1}^{L} \bar{\alpha}_i \|s_i\| + \sum_{i=1}^{L} \hat{\eta}_i e^{-\gamma_i t}$. Now, define $\tilde{\Theta}(t) = \sum_{i=1}^{L} \bar{\alpha}_i \|s_i\|$, we have

$$\begin{aligned} 0 \le V_D &= V_D(0) + \int_0^t \dot{V}_D dt, \\ &= V_D(0) + \int_0^t \left[-\tilde{\Theta}(\tau) \right] d\tau + \frac{\hat{\eta}_i}{\gamma_i} \left(1 - \hat{\eta}_i e^{-\gamma_i t} \right). \end{aligned} \qquad (52)$$

Since $V_D(0) + \frac{\hat{\eta}_i}{\gamma_i}\left(1 - \hat{\eta}_i e^{-\gamma_i t}\right) - V_D \ge 0$ and $\dot{V}_D \le 0$, hence $\lim_{t\to\infty} \int_0^t \tilde{\Theta}(\tau) d\tau$ exists and is finite (i.e. $\lim_{t\to\infty} \int_0^t \tilde{\Theta}(\tau) d\tau \ge 0$). Therefore, it follows from Barbalat's lemma (Gopalsamy, 1992) that $\lim_{t\to\infty} \int_0^t \tilde{\Theta}(\tau) d\tau = 0$ when $s_i(t) \to 0$ as $t \to \infty$. Thus, the proof of this proposition is achieved. □